DOI: 10.1111/tgis.12833

RESEARCH ARTICLE

Transactions in GIS WILEY

Fluvial inverse modeling for inferring the timing of Quaternary uplift in the Simbruini range (Central Apennines, Italy)

Michele Delchiaro[1] | Veronica Fioramonti[2] | Marta Della Seta[1] | Gian Paolo Cavinato[1,3] | Massimo Mattei[2]

[1]Department of Earth Sciences, Sapienza University, Rome, Italy

[2]Department of Sciences, Roma Tre University, Rome, Italy

[3]National Research Council, Office of Rome, Rome, Italy

Correspondence
Michele Delchiaro, Department of Earth Sciences, Sapienza University, Piazzale Aldo Moro 5, 00185 Rome, Italy.
Email: michele.delchiaro@uniroma1.it

Funding information
Ministero dell'Istruzione, dell'Università e della Ricerca, Grant/Award Number: PRIN_2015 (project 20158A9CBM_002)

Abstract

The timing of Quaternary uplift evolution of the Simbruini range (Central Apennines, Italy) is poorly known due to the lack of reliable chronological constraints of the post-orogenic continental clastic units, deposited after the upper Messinian thrust-top facies, and tectonic events. In this regard, we identified the main geomorphic markers, including several levels of continental units, whose plano-altimetric projection along the river longitudinal profile has been correlated with the main non-lithological knickpoints. Furthermore, we inferred the uplift history of the range by applying the inverse modeling of the river longitudinal profiles. Assuming a block uplift model, the drainage network cutting the Simbruini range recorded 2.4 ± 0.5 Ma of tectonic history, characterized by variable base-level fall rates (corresponding to variable uplift rates).

1 | INTRODUCTION

The topography of tectonically active regions shows a dynamic feedback between tectonics that moves rock masses, and surface processes that redistribute them from the hillslopes to the fluvial network shaping the landscape (Larsen & Montgomery, 2012; Montgomery & Brandon, 2002; Roering, Perron, & Kirchner, 2007; Willett, Slingerland, & Hovius, 2001). In this regard, bedrock streams, and more generally the entire fluvial system, are one of the most important agents that control the landscape evolution and are very sensitive recorders of

tectonic rate changes, allowing us to reconstruct the tectonic evolution where structural or geodetic data are unavailable (Howard & Kerby, 1983; Tucker & Whipple, 2002; Whittaker, Cowie, Attal, Tucker, & Roberts, 2007). Fluvial landscapes preserve features that reflect temporal and spatial variations in rock uplift rates, which are experienced as base-level changes (Delchiaro, Della Seta, Martino, Dehbozorgi, & Nozaem, 2019; Fox, Goren, May, & Willett, 2014; Gallen & Fernández-Blanco, 2021; Goren, Fox, & Willett, 2014; Ma, Zhang, Wang, Tao, & Li, 2020; Pritchard, Roberts, White, & Richardson, 2009; Roberts & White, 2010; Rudge, Roberts, White, & Richardson, 2015).

The study area is located in the Simbruini–Ernici range along the axial part of the Central Apennines. The Central Apennines developed since the Late Oligocene to present, as a consequence of the convergence and the following collision between the Africa and Eurasia plates (e.g., Carminati, Lustrino, Cuffaro, & Doglioni, 2010; Doglioni, Moretti, & Roure, 1991; Malinverno & Ryan, 1986). The long-term evolution of post-orogenic extensional tectonics in the Central Apennines is demonstrated by the presence of fault-bounded intermontane sedimentary basins (e.g., Fucino, Sulmona, L'Aquila, Rieti) that host thick stacks of continental deposits (e.g., Giaccio et al., 2015, 2019). These deposits have been dated using biostratigraphy and magnetostratigraphy, allowing for partial reconstruction of the onset and subsequent history of extensional tectonics in these sectors of the Apennines (e.g., Cosentino et al., 2017). The topographic growth was slow during the phase of major crustal shortening that occurred during the Miocene–Pliocene, but strongly accelerated in the Quaternary, when the shortening slowed down and the whole area was affected by strong uplift and extensional faulting striking mainly NW–SE (D'Agostino, Jackson, Dramis, & Funiciello, 2001; Molin & Fubelli, 2005).

The Simbruini–Ernici range represents one of the most important tectonic structures of the chain and its topographic relief, with deeply incised valleys, testifies to a significant local uplift. However, the timing and relevance of Quaternary tectonics in the range is far from being fully understood, despite the clear structural and geological evidence of normal faulting (e.g., Fabbi, 2018), which clearly dissects the Late Miocene to Early Pliocene compressional structures. In fact, in contrast with other sectors of the Central Apennines, this part of the chain lacks well-defined intermontane basins, except for the northern termination of the Simbruini ridge, the Oricola–Carsoli basin, which has recently been described in detail (D'Orefice et al., 2014). The post-orogenic tectono-sedimentary history is only recorded by several sedimentary cycles of alluvial and slope deposits, cropping out along the mountain slopes and on top of the relief, where they represent the relicts of paleosurfaces (e.g., Fabbi, 2018). Nevertheless, the study of these coarse-grained alluvial deposits is strongly hampered by the absence of fossils and other reliable stratigraphic and chronological data, and most of them have not been studied and mapped in detail, leaving the post-orogenic evolution of this sector of the chain substantially unknown (Bosi & Messina, 1990; Damiani, Catenacci, Molinari, Panseri, & Tilia, 1998; Devoto, 1967a, 1967b, 1970). Moreover, a river profile inverse model has not been applied to drainage in the region yet.

In this article, we present a geological and morphometric study of the area corresponding to the axial culmination of the antiformal central Simbruini range, where the history of post-orogenic extension has been characterized by the deposition of continental clastic deposits, whose remnants crop out at different heights above the present base level, as a consequence of strong uplift and river incision. The general purpose of this work is therefore to shed light on the final stages of the post-orogenic deformation in the central Simbruini range. To achieve this objective, it has been necessary to:

1. study, classify, and map the alluvial and slope deposits through detailed geological and geomorphological surveys;
2. project the relict basal surfaces of the different levels of the continental sequence along the main river longitudinal profiles, in order to identify the most important phases of the regional morpho-evolution; and
3. reconstruct the uplift history of the range through the fluvial inverse modeling.

2 | GEOLOGICAL SETTING

The Simbruini Mts. are located in the axial sector of the Central Apennines (Figure 1), a fold-and-thrust belt forming a chain–foredeep–foreland system progressively migrating towards the east during the late Miocene–Pliocene times as a consequence of the slab rollback of the subducting Adriatic lithosphere (Accordi, 1966; Bally, 1986; Castellarin, Colacicchi, & Praturlon, 1978; Cavinato, Corrado, & Sirna, 1993; Cipollari & Cosentino, 1999; Elter, Giglia, Tongiorgi, & Trevisan, 1975; Funiciello & Parotto, 1978; Martinis & Pieri, 1964; Parotto, 1980; Parotto & Praturlon, 1975; Patacca & Scandone, 1987). The structural architecture of the chain has been substantially complicated by post-orogenic extensional tectonics, which affected the Central Apennines area since the late Miocene and have been responsible for the basin and range morphology of the chain. Extensional tectonics in the Apennines has been accommodated by normal faults, which bound extensional sedimentary basins whose age becomes progressively younger from the Tyrrhenian coast to the east, towards the axial part of the chain, where normal faults are now still active (Kastens & Mascle, 1990; Lavecchia, Brozzetti, Barchi, Menichetti, & Keller, 1994; Malinverno & Ryan, 1986; Sartori, 1990).

The Simbruini Mts. represent a typical structure of the Central Apennines area, both in terms of stratigraphy and tectonic evolution (Figure 1a). They are formed by a marine succession extending from Upper Triassic to Upper Miocene, which underwent different episodes of thrusting and folding time-constrained by the presence of different syn-orogenic and thrust-top deposits (Carminati, Fabbi, & Santantonio, 2014; Cavinato & DeCelles, 1999; Cipollari & Cosentino, 1993, 1995; Cipollari et al., 1999; Fabbi, 2016, 2018; Ghisetti & Vezzani, 1997; Patacca, Scandone, Di Luzio, Cavinato, & Parotto, 2008). The Mesozoic stratigraphy is characterized by about 4,000 m of an Upper Triassic to Upper Cretaceous carbonate succession (Chiocchini, Chiocchini, Didaskalou, & Potetti, 2008; Damiani, 1990; Devoto, 1967a, 1970; Devoto & Parotto, 1967; Parotto & Praturlon, 1975, 2004), followed by a "Paleogene hiatus" and by Miocene carbonate ramp deposits (Brandano, 2002; Cipollari & Cosentino, 1995; Civitelli & Brandano, 2005; Cosentino, Cipollari, Marsili, & Scrocca, 2010; Damiani, Catenacci, Molinari, & Pichezzi, 1991). The carbonate sedimentation ceased during the late Miocene when the Simbruini Mts. area was characterized by a gradual transition to foredeep conditions, which caused the drowning of the carbonate ramp and the deposition of hemipelagic marls and siliciclastic turbidites, extensively outcropping in the Roveto valley to the east (Carminati, Corda, Mariotti, & Brandano, 2007; Cipollari & Cosentino, 1991; Critelli et al., 2007; Fabbi, Galluzzo, Pichezzi, & Santantonio, 2014; Milli & Moscatelli, 2000; Patacca & Scandone, 1989). Along the eastern side of the Simbruini Mts., the siliciclastic units are intercalated in their lower part with psephitic facies, the "Brecce della Renga," which reflects tectonic-driven dismantling of submarine escarpments bordering prominent structural high and submarine sedimentation, related to the occurrence of a late Miocene, pre-orogenic, extensional tectonic phase in the area. This paleogeography was probably related to the presence of pre-orogenic normal faults that, during the foreland bending, formed Cretaceous and Miocene carbonate structural highs (Compagnoni, Galluzzo, & Santantonio, 1990; Fabbi & Rossi, 2014). The latter were progressively eroded and became the main source-rocks area of the "Brecce della Renga Fm." succession (Carminati et al., 2014; Fabbi, 2012, 2016, 2018; Fabbi et al., 2014; Fabbi & Rossi, 2014).

The last remnants of Miocene sediments in the Simbruini axial sector crop out on the western side of the Viglio Mt. and in other limited areas across the Simbruini range (thrust-top units, Figure 1b; Cavinato, Parotto, & Sirna, 2012; Cipollari & Cosentino, 1993; Fabbi & Santantonio, 2019). In this sector, the clays and conglomerates, which unconformably overlie the deformed pre-orogenic and syn-orogenic units, represent the last sedimentary cycle involved in compressional deformation (Cavinato et al., 2012; Cipollari & Cosentino, 1999; Cosentino et al., 2010). These pelitic and psephitic–psammitic deposits (i.e., "Argille con Robulus" and "Puddinghe poligeniche" near Colle Cenciarella and Fonte della Moscosa localities, Figures 2a,c, respectively; Devoto, 1970) have been attributed to clastic sedimentation in environments ranging from fluvial, marshy-lacustrine to coastal, generated during the formation and migration of the thrust-top basin, and mark the last episode of marine sedimentation in

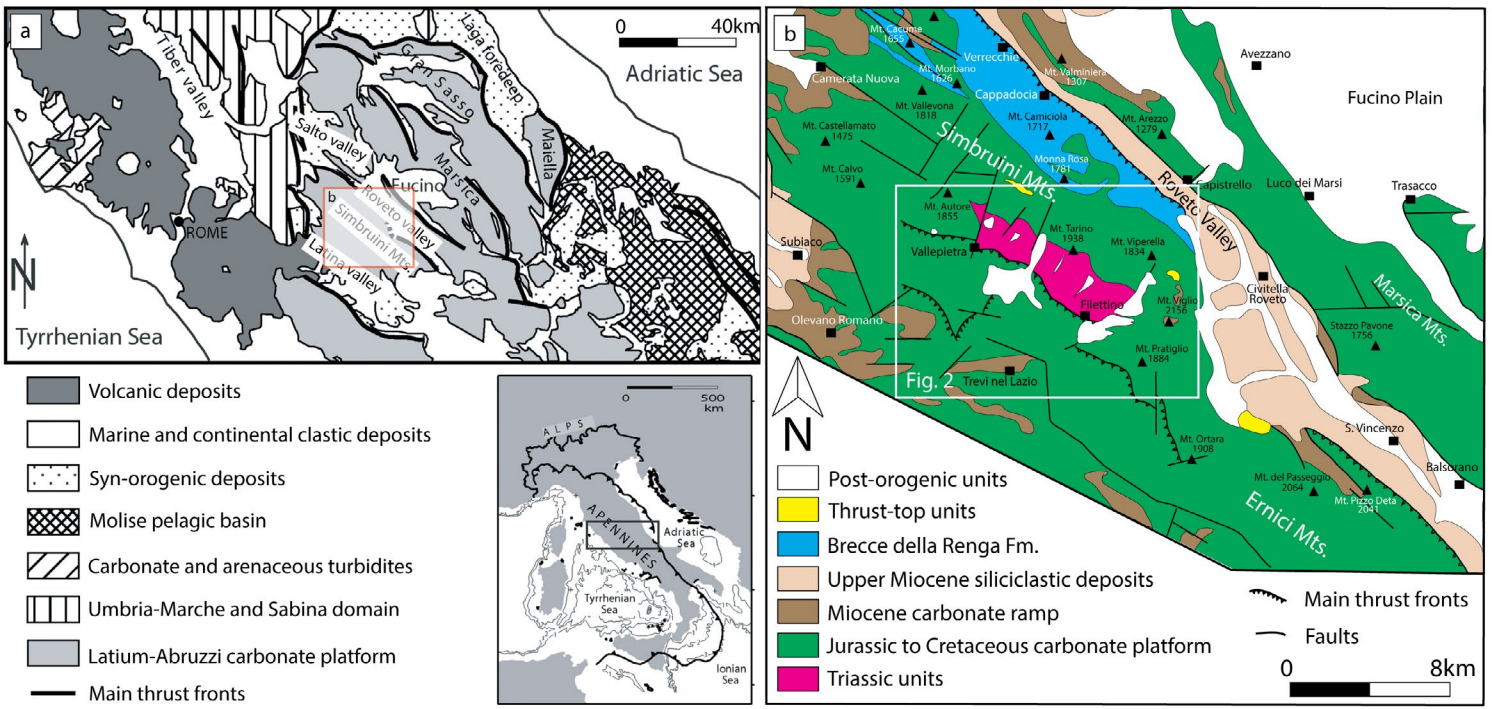

FIGURE 1 (a) Geological schemes of the Central Apennines; and (b) the Simbruini–Ernici range. The location of Figure 2 is reported as well (modified from Carminati et al., 2014; Fabbi & Rossi, 2014)

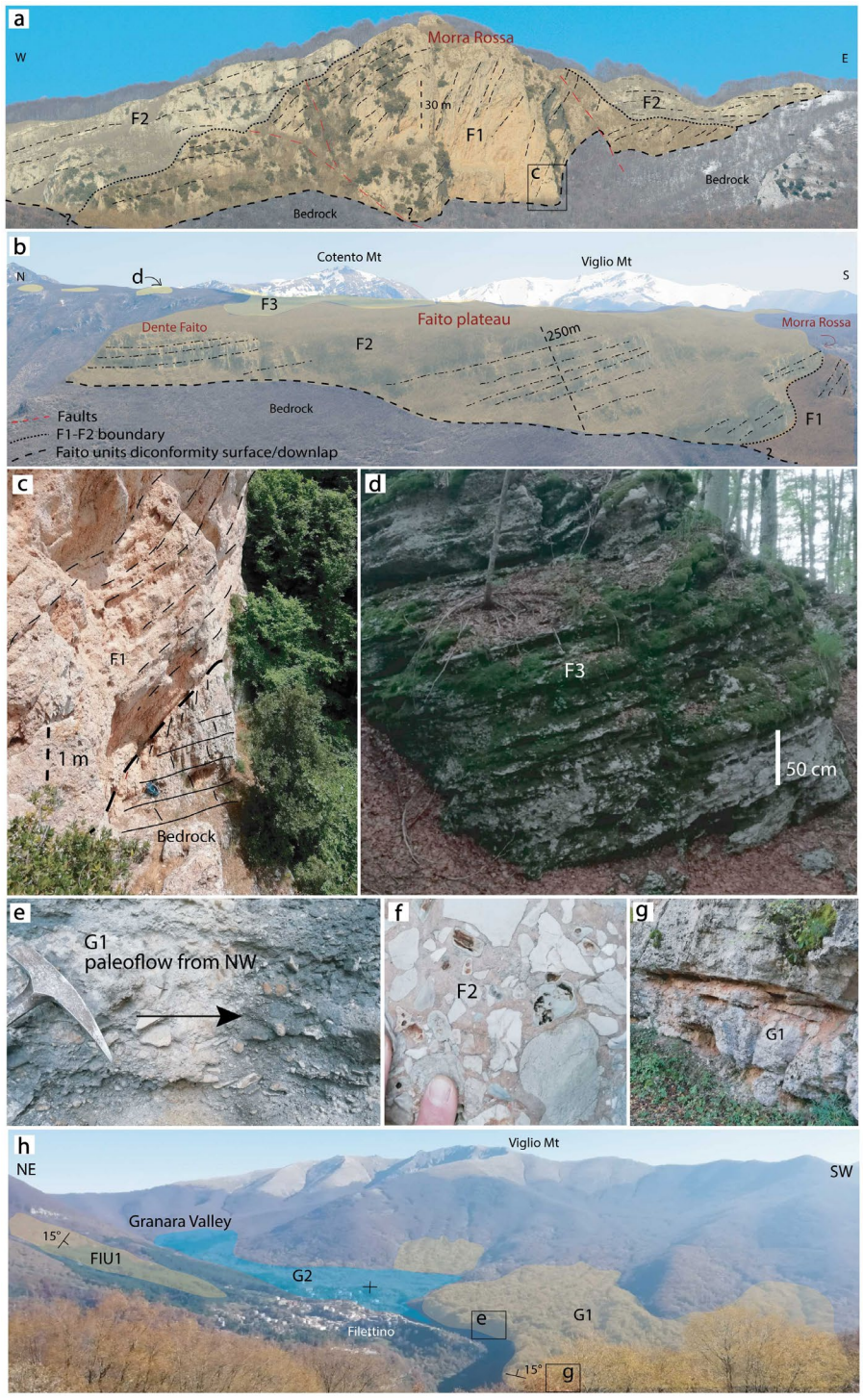

FIGURE 2 (a) Hillshade map of the study area in which the outcrops of the continental clastic deposits, the related ordered points (in correspondence with the erosive base outcrop), the knickpoints, and the geological sections are shown. (b) Zoom on the Faito and Simbrivio sequences. (c) Zoom on the Granara and Fiumata sequences. (d)–(f) Geological cross-sections of the Faito, Granara, and Fiumata suites. The coordinate system is WGS84-33N, EPSG: 32633. The hillshade map is derived from the 10 m-resolution TINITALY DEM (Tarquini & Nannipieri, 2017)

the area (Accordi et al., 1967; Cavinato et al., 2012; Cipollari & Cosentino, 1999; Cosentino et al., 2010; Fabbi & Santantonio, 2019; Pasquali, Castorina, Cipollari, Cosentino, & Lo Mastro, 2007).

The tectonic structure of the Simbruini Mts. is characterized by a homocline of Upper Triassic to Upper Cretaceous carbonate deposits, dipping to the east, that in the eastern side of the range is folded and thrusted onto the Upper Miocene siliciclastic units of the Roveto valley. Definitive evidence of the tectonic duplex of the Simbruini Mts. is given by the "Trevi 1" well data, where the Triassic carbonates outcropping at the core of the structure are superimposed on Cretaceous carbonates and Upper Miocene marls (Dondi, Papetti, & Tedeschi, 1966). The fold-and-thrust structures are mainly NW–SE striking and NE verging. Locally, the thrust planes strike N–S, defining an arcuate geometry of the structures like the one clearly exposed in the Roveto valley (Devoto, 1967; Parotto, 1971). The Simbruini Mts. are also characterized by the occurrence of anomalous tectonic contacts (low-angle faults with younger-on-older relationships) recognized along the Vallepietra–Filettino–Monte Ortara alignment (Beneo, 1938; Cosentino et al., 2010; Dondi et al., 1966; Parotto, 1971). This structure is parallel to the Simbruini thrust front, is located in the middle of the Simbruini ridge, and has a complex transpressive kinematics (Naso, Parotto, Tallini, & Tozzi, 1992). Along this lineament, dipping 45°–60° to the SW, Cretaceous carbonate units tectonically overlie Jurassic and Upper Triassic deposits (Damiani et al., 1998; Devoto, 1967a, 1967b; Devoto & Parotto, 1967; Pieri, 1966). The presence of syn-orogenic and thrust-top deposits allowed constraining the age of compressional episodes in the Simbruini range in the Messinian–Early Pliocene, when these units were deformed by several episodes of thrusting (Cavinato et al., 2012).

The orogenic phases caused uplift and emersion of this sector of the Central Apennines, and were followed by SW-directed extensional tectonics, with NW–SE trending, SW dipping, normal faults, dissecting the fold-and-thrust structures and producing the progressive down-throwing of the stratigraphic succession in the western sector of the Simbruini range.

The study area is located at the core of the antiformal structure of the Simbruini Mts. and is characterized by a complex structural architecture and by a high local topographic relief. The outcropping geology of the area is synthesized in Figure 1b and consists of a Mesozoic bedrock unconformably covered, in its eastern side, by Upper Miocene carbonate clastics ("Brecce della Renga" Fm.), hemipelagic and foredeep siliciclastic units, and, with another angular unconformity, polygenic psephitic–psammitic deposits ("Puddinghe Poligeniche"), which represent the last marine units in the area. The outcropping deposits are arranged in two main tectonic units separated by a regional low-angle fault. The lower tectonic unit is formed by a homocline dipping to NE, made of Triassic–Jurassic units. The upper tectonic unit is mostly formed by Cretaceous carbonates, generally dipping to the NE. The nature of the "Vallepietra–Filettino" fault, characterized by younger-on-older geometry, has largely been debated in the scientific literature and has been interpreted as: (1) a thrust fault which involved an already deformed structure (Parotto, 1971); (2) a thrust fault which was reactivated as a normal fault (Cosentino et al., 2010); or (3) a low-angle extensional detachment fault (Calamita, Di Domenica, Viandante, & Tavarnelli, 2008). The tectonic structure of the area is further complicated by the presence of high-angle normal faults, dipping to the SW, which dissect the homocline in a sequence of fault-bounded tilted blocks which progressively lowered the entire structure to the SW, where the upper portion of the stratigraphy is preserved.

In this framework, due to a lack of intermontane basins, the last recorded sedimentary event is represented by several cycles of continental clastic deposits, resulting from the intense fluvial erosion of the carbonate deposits. The landscape evolution in subaerial conditions started diachronically and is testified by the remnants of clastic deposits at different heights above the present-day base level of the drainage network.

A precise evaluation of regional uplift rates in the Middle–Late Pleistocene is hampered by the relative scarcity of remnant shoreline deposits and uncertainties in their ages, especially on the Adriatic coast. Nevertheless, approximate long-term uplift rates have been estimated by Bigi et al. (1995) in the order of 0.3–0.5 mm a^{-1} in the last 1 Ma, based on the present maximum elevation (480–500 m) of the Lower Pleistocene shorelines and associated deposits. Similar values (0.1–0.26 mm a^{-1}) can be estimated for the long-term uplift on the Tyrrhenian side based on the elevation (~200–400 m) of the Early Pleistocene shoreline (~1.8–2.6 Ma). These rates are likely to be higher

along the axis of the Apennines itself (D'Agostino et al., 2001; Molin & Fubelli, 2005), as reported also by Girotti and Piccardi (1994), suggesting 0.5–0.7 mm a^{-1}.

3 | POST-OROGENIC DEPOSITS

The study of the continental coarse-grained clastic deposits outcropping in the Simbruini range had been strongly hampered by the scarcity of sufficiently detailed and reliable stratigraphic data. The continental nature of these deposits is clearly demonstrated by the pink to reddish color of the matrix, by the carbonatic cement related to meteoric water circulation, and by the sporadic finding of ostracod as only fossil content. Most of these deposits are still to be studied, mapped, and dated in detail, despite their depositional history being crucial for providing chronological constraint on the history of Quaternary tectonics in the Central Apennines (Damiani et al., 1998; Devoto, 1967a). For these reasons, we performed a detailed geological and geomorphological survey in order to sample and genetically classify the continental deposits. In this section we describe the analyzed clastic deposits related to the post-orogenic history of this sector of the Simbruini range (Figure 2).

The study area, comprised among Trevi nel Lazio, Vallepietra, and Filettino, is characterized by the presence of a huge amount of continental coarse-grained, mainly carbonatic, deposits (Accordi & Carbone, 1986). Here, the combined effects of uplift, normal faulting, and climatic oscillations strongly influenced the landscape evolution (Accordi & Carbone, 1986).

The landscape evolution in subaerial conditions is testified by the remnants of clastic deposits hanging at different elevations, from about 800 m on the Aniene valley bottom, near Trevi nel Lazio village, to 1,600 m on top paleosurfaces (Figure 2a). The most relevant clastic deposits crop out in correspondence to the Faito plateau, which rises between Vallepietra and Filettino villages (Figure 2b). Other relevant deposits lie scattered on both sides of the Simbrivio and Aniene valleys, at lower elevation with respect to the Faito ones (Figure 2c). All the deposits lie unconformably on the pre-orogenic Mesozoic bedrock, show different degrees of weathering by exogenous agents, and underwent a different degree of karstification. Moreover, the contribution of glacialism in the Plio-Pleistocene landscape evolution of the Simbruini Mts. was studied extensively in the past by Bieler-Chatelan (1928, 1929), Damiani and Pannuzi (1976, 1980, 1990), and Jaurand (1994). Traces of glacial modeling relating to the last glaciation are evident, along the slopes of Viglio, Cotento, and Tarino Mts., where numerous glacial cirques outcrop. Furthermore, Campo Catino (Figure 2) has been interpreted as of glacial origin, since it is partly occupied by morainic deposits and dotted with erratic boulders (Damiani & Pannuzi, 1976, 1980, 1990; Jaurand, 1994). Nevertheless, all the deposits described in the following subsections are referred to fluvial processes.

3.1 | Faito plateau

The Faito plateau (Figure 2b) covers an area of about 6 km^2 and lies among the deeply incised Simbrivio, Fiumata, and Granara valleys, at an elevation ranging between 1,442 m in the southern area and 1,676 m to the north (near Tarinello Mt.).

The origin of these deposits has been studied by Beneo (1938) and Devoto (1967a), who considered them Quaternary in age because of their continental nature. Damiani (1990, 1998), on the other hand, hypothesized a correlation with the "Brecce della Renga Fm.", which crops out extensively on the eastern slope of the Simbruini range and which has later been recognized as a lower Tortonian–lower Messinian marine clastic unit, resulting from the sedimentation along the margins of the Simbruini structural high, developed as a result of the early Tortonian extensional tectonics (Fabbi & Rossi, 2014).

Based on their texture, geometric relationships, and petrographic observations, the Faito clastic deposits have been subdivided into three sub-units: F1, F2, and F3 (Figures 3a–d).

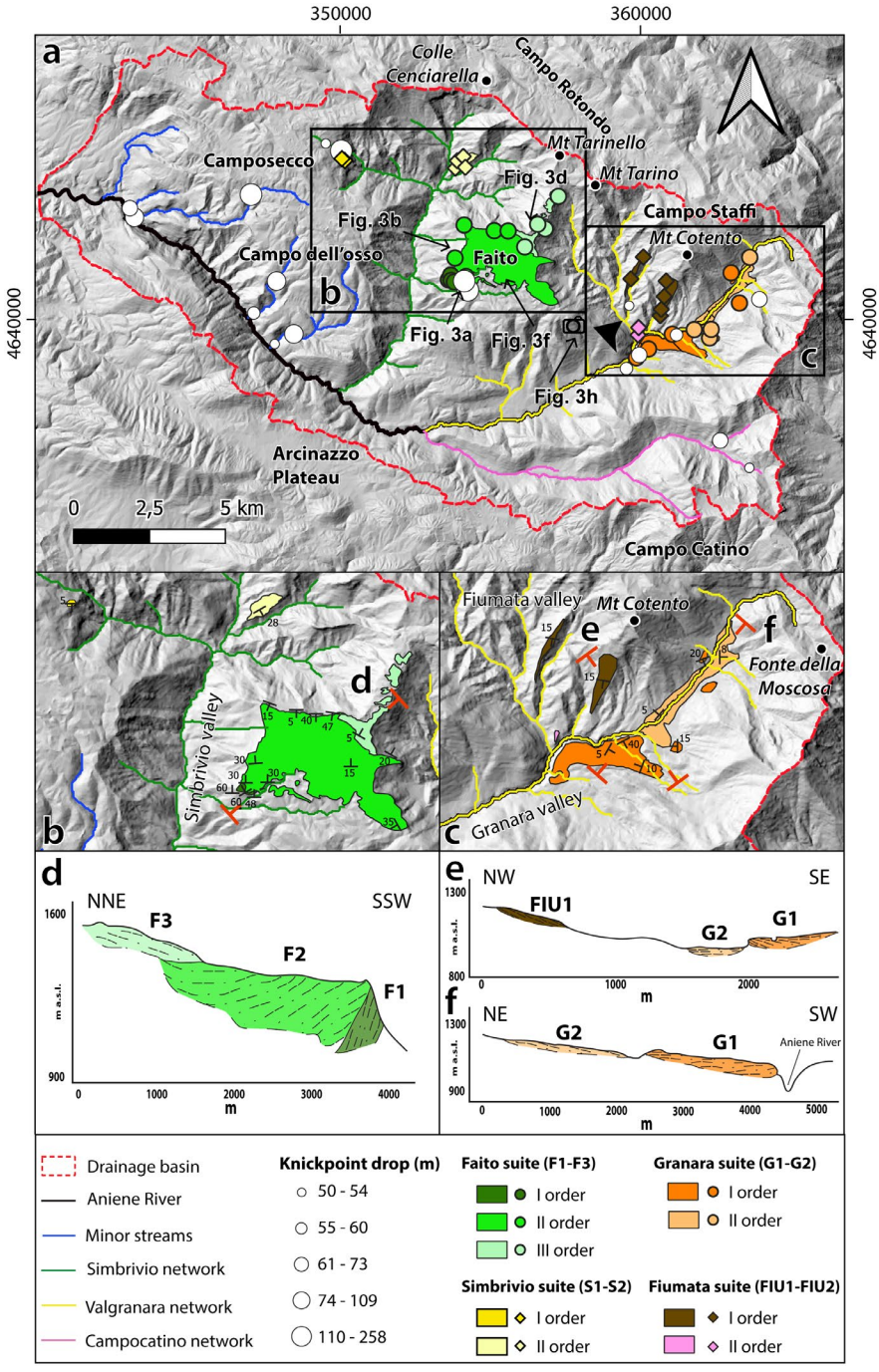

FIGURE 3 Photos taken during the field survey. (a) The spectacular morphology of the south side of the Faito plateau consisting of bedrock cliffs and overhangs, localized in correspondence with the disconformity boundary with the cretaceous bedrock, where F1 proximal facies crop out. (b) West side of the Faito plateau in a N–S panoramic view with the layering of the breccia deposits clearly visible. (c) Detail of the very steep beds, clast-supported and heterometric F1 unit, and the boundary with the bedrock. (d) Faito's F3 unit, well organized, with cross-laminations and channelization features. (e) Detail of clast embracement in G1 unit (Granara valley). (f) Close-up on the matrix-supported texture of F2 Faito's breccia. (g) G1 Granara deposit—layers dip in the opposite direction to the present-day slope. (h) Panoramic view of Granara valley. See Figure 2 for locations

F1 is the oldest cycle and is well visible to the south of the Faito plateau (Figures 3a,b). It rests unconformably on top of Cretaceous limestones and Jurassic dolostones (Figures 3a,b). The deposits of the F1 cycle are well cemented, with irregular beds 60–120 cm thick. The beds are dipping about 60° toward the north, and are composed of clast-supported, heterometric, carbonate breccias mostly made up of Upper Cretaceous limestones (Figure 3c). Clast size ranges from centimetric to plurimetric, with angular aspect. The average thickness of the F1 sub-unit is 80 m. The F1 cycle is clearly cut and tilted by a NW–SE oriented normal fault system.

The F2 sub-unit, which represents the main deposit of the Faito plateau, rests with a disconformity on top of the F1 sub-unit and Mesozoic bedrock. The basal disconformity is characterized by a slightly marked red surface, clearly observable at the contact with both the F1 cycle and Mesozoic bedrock. The F2 sub-unit has a thickness of about 250 m. In the lower portion the deposit is generally well cemented, massive, or poorly stratified, and poorly sorted. In the upper part, the F2 sub-unit becomes more organized, with well-defined bedding, 20–40 cm thick, also showing cross-laminations. The F2 sub-unit shows a gentle tilting (20°–40°) to N–NNE (Figure 3b).

Different from F1, F2 shows an alternation of clasts and matrix-supported layers. The clasts are sub-angular to sub-rounded, with size ranging from millimetric to centimetric (Figure 3f), with a minor content of larger cobbles. The analysis of the clast composition shows that the F2 sub-unit is mostly made by Cretaceous carbonate rocks. The F2 sub-unit is also cut and tilted by a NW–SE normal fault system.

At higher elevation, in the northern sectors of the plateau, the younger cycle F3 crops out, representing the development of an alluvial fan system. The F3 cycle is in stratigraphic contact both with F2 and Cretaceous and Jurassic limestone/dolostone (Figure 3b). The bedding shows local variations, from sub-horizontal to a few degrees of inclination to north and south. The deposit is well cemented, very porous, generally well organized, with cross-laminations and channelization features, and represents the development of an alluvial fan system (Figure 3d). The clast size ranges from millimetric to centimetric, mainly sub-angular, rarely sub-rounded in aspect. Clast content is made up mostly of dolostones with a lower content of limestones, both deriving from the Mesozoic carbonate substratum. The average thickness has been estimated at about 80 m, but is extremely variable and discontinuous.

The Faito deposits lie at the top of isolated mountains, disconnected from their source, like “remnants” of old relict clastic sedimentary bodies. The contact with the bedrock follows the mountainside and describes a complex paleotopography. In general, the Faito plateau deposits fill a N–S oriented wide synclinorium, related to a relict landscape, today obliterated. This hypothesis is also suggested by the findings of a similar deposit on the other side of the Simbrivio valley, at the same height and resting with a disconformity on the Cretaceous limestone (S1 unit, discussed later). These deposits crop out in correspondence with the Campo dell’Osso relict surface, with a setting similar to the one observed in the Faito plateau. These relict surfaces are widely distributed in the area (i.e., “Campo dell'Osso,” “Camposecco,” “Campo Rotondo”), as shown in Figure 2.

3.2 | Granara, Fiumata, and Simbrivio valleys

Along the sides of the Granara, Fiumata, and Simbrivio valleys, at lower elevation with respect to the Faito plateau, different slope and alluvial fan clastic deposits crop out, distributed on both sides of the valleys, with a thickness ranging from 50 m up to at least 150 m (Figures 3g,h).

The stratigraphy and age of the continental deposits of the Granara valley are still unclear and several interpretations have been proposed in the past (Beneo, 1938; Damiani, 1990; Devoto, 1967). The newly collected data allowed us to discriminate different sedimentary cycles, which show different clast lithology and relationships with the present-day topography.

To the north of Filettino village, the FIU1 unit crops out (between 1,050 and 1,454 m a.s.l.) in two isolated ridges along the western slope of the Cotento Mt. (Fiumata valley), directly overlying the Jurassic/Triassic limestones and dolostones. The deposit is well cemented and very porous, generally well organized, in layers 10–60 cm thick, with cross-laminations and channelization features. The layers are mostly clast-supported and sometimes

show normal grading. Clasts are commonly sub-angular, rarely sub-rounded. The samples collected are mainly composed of dolostones (which are prevailing in the Jurassic and Lower Cretaceous stratigraphy) with a lesser content of limestones, similar to the Faito F3 sub-unit. Clasts are commonly sub-angular, rarely sub-rounded, especially in correspondence with the matrix-supported layers.

Toward the bottom of the Fiumata valley, near Filettino village, the FIU2 clastic unit crops out between 889 and 936 m a.s.l. The outcrop is very limited in extent and made of clast-supported and heterometric carbonate clasts. FIU2 has been interpreted as an alluvial fan deposit ascribed to the recent evolution of the Fiumata valley, according to its location (it lies at the bottom of the valley) and water flow directions derived from imbrications.

To the south and southeast of Filettino village, on the left-side slope of Granara valley, the G1 unit crops out between 905 and 1,200 m a.s.l., directly above the Mesozoic limestones and dolostones. The clastic deposit is deeply karstified and crops out in suspended terraced bodies. The deposit is almost 80 m thick and presents different bed attitude. Near the contact with the bedrock, the clastic deposit is organized in beds 40–80 cm thick with dip direction opposite to the present-day slope. Clasts are angular, centimetric to decametric. Flow directions from the SW and NW have been identified in the lower part of the deposit (Figure 3e). Toward the top, the deposit becomes less inclined, more stratified, with an increase in the internal organization and matrix content. Clast dimension is millimetric to decametric, with mostly angular aspect. Clasts are composed exclusively of Mesozoic carbonate, mainly dolostones with a lesser content of limestones. The sedimentological features of this unit led to its interpretation as forming a debris cone evolving upward to a mixed debris flow/alluvial fan deposit.

Around Filettino village, at the bottom of the Granara valley (between 1,240 and 978 m a.s.l.), the G2 deposit crops out, within the incised terraces of the G1 deposits. The G2 deposits can easily be distinguished from G1 because they are polygenic, with clasts deriving from the Mesozoic carbonate platform and from the Messinian "Puddinghe Poligeniche." The deposit has an average thickness of 50 m, is sub-horizontal with decametric to metric beds, generally well cemented, very heterometric, and generally clast-supported. Clasts ranges from millimetric to decametric, from angular to sub-rounded. Flow direction indicates a close connection with the present-day valley morphology and relief. This deposit is younger than the G1 unit, for several reasons: (1) it lies at the bottom of the valley; (2) it infills the valley incised in the G1 deposit; and (3) it shows flow direction from N to NE, following the present-day valley morphology and from a source area where the "Puddinghe Poligeniche" crops out.

In the context of Simbrivio valley, two deposits have been detected: (1) a terraced one which crops out north of Vallepietra (S2); and (2) a minor one cropping out on top of the valley, near the Campo dell'Osso relict surface, at the same height but on the other side of the valley from the Faito plateau (S1, Figure 2b).

To the north of the "Campo dell'Osso" relict surface, at 1,443 m a.s.l., the S1 deposit crops out, hanging on the Simbrivio valley bottom. The clastic deposit is very porous, sub-horizontal, and poorly stratified. Despite the extremely weathered aspect of the deposit, a matrix-supported level was detected, which is characterized by a pink calcarenitic matrix, such as the Faito plateau deposits. The total thickness of the deposit does not exceed 15 m. The clasts are mostly angular and derive from the local Mesozoic succession. Due to the strong weathering of the deposit, it is not possible to make many considerations, but the elevation and nearness to Faito units suggests a possible age correlation with these deposits, and hints that the Faito units could be part of a more extensive landscape unit, eroded during the formation of the Simbrivio gorge.

S2 crops out between 899 and 970 m a.s.l. The contact with the underlying Triassic dolostones is sharp. It has been interpreted as a slope breccia, since it is very heterometric and chaotic, well cemented and mostly clast-supported, in beds with a thickness comprised between 20 and 80 cm. Layers with a matrix-supported texture are rarely observed and could be associated with debris flow events fed by the same slope deposits. Clasts vary from millimetric to metric, from angular to rounded in aspect. The macroscopic observation revealed only the presence of clasts belonging to the Mesozoic carbonate platform.

4 | PROJECTIONS OF THE GEOMORPHIC MARKERS

The best geomorphic markers preserved in the study area are represented by the continental clastic deposits identified during the field survey, including the Faito (F1–F3), Simbrivio (S1, S2), Granara (G1, G2), and Fiumata (FIU1, FIU2) suites. In detail, we refer to the relict basal surfaces of the deposits as markers of the morpho-evolutive erosive phases.

We investigated the plano-altimetric distribution of the main geomorphic markers represented by the continental deposits identified during the field survey, as well as the main non-lithological knickpoints along the river longitudinal profiles of the valleys cutting the Simbruini range, included in the upper Aniene river drainage basin. The drainage network was extracted from the 10 m-resolution TINITALY digital elevation model (DEM) (Tarquini & Nannipieri, 2017) and analyzed using TopoToolbox, a set of Matlab functions for topographic analysis (Schwanghart & Scherler, 2014) and the Topographic Analysis Kit (TAK) by Forte and Whipple (2019). Major river systems were extracted that drain the upper valley of the upper Aniene river basin, where the drainage area exceeds 10^6 m^2. Specifically, the TAK function "ProjectOntoSwath" was used to project points (from basal surfaces of geomorphic markers) on the river longitudinal profiles. The knickpoints were detected using the TopoToolbox function "knickpointfinder," with a tolerance value of 30 m. This value reflects uncertainties associated with longitudinal river profile data, as it is higher than the maximum expected error between the measured and the true river profile.

4.1 | Results

A plano-altimetric analysis of the major knickpoints distinguished based on their elevation drop, as well as the geomorphic markers identified during the field survey, was conducted (Figure 4). The knickpoint histogram in Figure 4b shows quite well a cluster correlating with the highest clastic deposits (between 1,550 and 1,300 m a.s.l.) that are associated with the presence of a large anomalous patch of low-relief/slope landscape. The low-relief areas are especially visible in the Vallepietra, Granara, and Campocatino networks, elevated by at least 700 m above the Aniene trunk channel, and have low-slope hanging reaches with increasing vertical drop toward downstream segments (Figure 4). The histogram also shows two other minor knickpoint clusters at elevations of 1,000–800 and 600–400 m a.s.l., respectively, in the Granara, where the G1 and G2 breccias crop out, and along the lower reach of the upper Aniene river valley.

Specifically, it is possible to observe that the Faito suite encompasses the morphology of the plateau with a decreasing slope from F1 to F3. The F1 deposits appear tilted with dip angles from 60 to 30°, while the F2 deposits are characterized by 47–5° and F3 by 35–5°. Since the deposit basal surface is erosive, it is possible to assume that the low-relief morphology was formed during the F3 emplacement, and the erosive wave associated with the knickpoint cluster between 1,550 and 1,300 m a.s.l. has started subsequently. Moreover, S1 fits very well, respectively, with the F2 projection and the S2 deposits with the two minor clusters of the knickpoint. While along the Granara valley network, the projections marked the second phase of the erosive wave passage. It is important to note that the deposit dip angles range from 40 to 5° and appear undeformed. In detail, the FIU1 deposits lie above a quite steep slope, indicating that they are probably associated with debris flow/debris cone emplacement in the hillslope domain. The G1 deposits are at higher elevations, while the last recorded impulse of the erosive wave was followed by the deposition of FIU2 and G2 suites that are correlated with the minor knickpoints between 1,100 and 800 m a.s.l.

5 | FLUVIAL INVERSE MODELING

To infer the uplift history of the Simbruini range, we applied the stream power law (SPL) equation system (Howard & Kerby, 1983). In detachment-limited conditions, typical of tectonically active regions, the evolution of the river

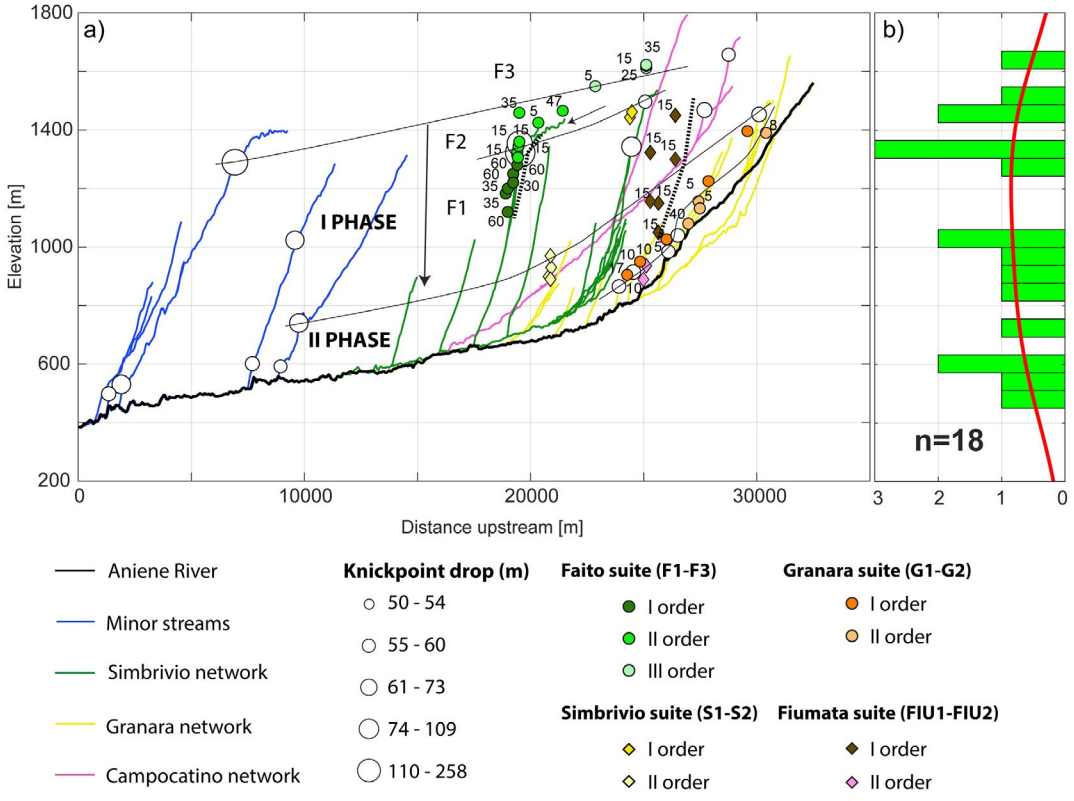

FIGURE 4 (a) The longitudinal profiles of all the stream networks (including Simbrivio, Granara, and Campocatino sub-catchments) of the upper Aniene river basin along which the knickpoints and the erosive base outcrops of the identified continental clastic sequences are projected. Moreover, dips related to the projected clastic deposits are shown. (b) The knickpoint elevation histogram is reported

profile is described as the change in elevation z of a channel point x through time t (Howard & Kerby, 1983), which relates to the competition between erosion (E) and uplift (U):

$$\frac{dz(x,t)}{dt} = U(x,t) - E(x,t) \tag{1}$$

where the fluvial erosion E is computed as:

$$E(x,t) = KA(x)^m \left(\frac{dz(x,t)}{dx}\right)^n \tag{2}$$

The powers m and n are positive constants controlling the erosion mechanism. Specifically, m depends on the climatic conditions and hydraulic properties of the discharge, and n is a function of other erosional thresholds (Di Biase & Whipple, 2011; Whipple & Tucker, 1999). The erodibility, K, accounts for the lithology, the climatic conditions, and the channel geometry. In the general case, K can vary in space and time, but in the treatment presented here, it is taken as a constant, as it is representative of the long-term evolution of climatic and lithologic conditions (e.g., Lague, 2014). Indeed, since there are no independent constraints on this parameter in the study area, it is not possible to define its variation over time. According to the steady-state conditions, the surface elevation is the

resulting equilibrium between the erosion rate and the relative uplift rate, $U(x, t) = E(x, t)$. A power-law relationship between the local channel slope (S) and the upstream drainage area (A) reveals the steady-state river profile:

$$S(x,t) = \left(\frac{E(x,t)}{K}\right)^{\frac{1}{n}} A(x)^{\frac{m}{n}} = k_{sn} A(x)^{-\theta} \tag{3}$$

where $k_{sn} = (E(t, x)/K)^{1/n}$ is known as the steepness index and the mn ratio, or θ, is defined as the concavity index. When $n = 1$, the steepness index takes the form (Kirby & Whipple, 2012):

$$k_{sn} = \frac{E(x,t)}{K} = \frac{U(x,t)}{K} \tag{4}$$

If U and K are space-invariant, we can perform the integration of $(U/K)^{1/n}$ from a base level x_b to an arbitrary upstream point x of the channel to predict the elevation of a river profile (Perron & Royden, 2013):

$$z(x) = z(x_b) + \left(\frac{U}{KA_0^m}\right)^{\frac{1}{n}} \chi \tag{5}$$

where A_0 is an arbitrary scaling area and χ is an integration of river horizontal coordinates defined by the equation

$$\chi = \int_{xb}^{x} \left(\frac{A_0}{A(x')}\right)^{\frac{m}{n}} dx' \tag{6}$$

The erosional wave celerity $C(x) = KA(x)^m S(x)^{n-1}$ controls the speed at which perturbations travel along the channel (Whipple & Tucker, 1999). The response time $\tau(x)$ for perturbations to propagate from the river outlet, at $x = 0$, to a point x along the channel is expressed as (Whipple & Tucker, 1999):

$$\tau(x) = \int_0^x \frac{dx'}{C(x')} = \int_0^x \frac{dx'}{KA(x')^m S(x')^{n-1}} = \frac{(x)}{KA_0^m} \tag{7}$$

where x' is an integer variable. The response time $\tau(x)$ increases constantly with x, from the base level to the high channel reaches. The τ-plot is the starting point for the linear inverse scheme to study the rock-uplift/base-level fall history recorded in the fluvial topography (Di Biase & Whipple, 2011; Whipple & Tucker, 1999). The mathematical expression of the current river elevation can be reported as (Goren et al., 2014):

$$z(x) = \int_{-(x)}^{0} U^*(t^*)\, dt^* \tag{8}$$

where

$$t^* = KA_0^m t \text{ and } U^* = \frac{U}{KA_0^m} \tag{9}$$

The parameters t^* and χ are in units of length, and U^* is a dimensionless rate of rock uplift. Along the channel profile on the χ–z plot, the slope of different channel segments represents the corresponding channel steepness (k_{sn}). To reintroduce time, the equations should by scaled by K. Indeed, the recession rate of knickpoints within the drainage basin is strongly dependent on the erosional coefficient K and the n exponent, as well as the drainage area (Di Biase & Whipple, 2011; Gallen, 2018; Goren et al., 2014; Whipple & Tucker, 1999; Wobus et al., 2006).

In this regard, spatially constant K and U were assumed as in a block uplift scenario employing the inverse approach stream power model solution proposed by Goren et al. (2014) and Gallen (2018). Moreover, a linear dependency between the local slope S and the erosion rate E in the stream power erosion model was assumed according to Equation (3) (i.e., the slope exponent $n = 1$ and the drainage area of the fluvial channels was kept fixed during the history, represented by the long profiles of the rivers).

5.1 | Parameter setting

The drainage network was extracted from the 10 m-resolution TINITALY DEM (Tarquini & Nannipieri, 2017) with a flow accumulation threshold for the fluvial domain at 10^6 m^2. Then, the following assumptions were made.

1. A linear dependency between the local slope S and the erosion rate E in the stream power erosion model was assumed, considering $n = 1$. It means that an advection equation predicting the parallel retreat of knickpoints at a celerity depending on erodibility and drainage area as in Equation (7) is considered suitable for the purpose of this study. However, when $n \neq 1$, the celerity becomes dependent on slope and the knickpoint geometry is altered as it propagates (Finnegan, Sklar, & Fuller, 2007; Lague, 2014; Tucker & Whipple, 2002). If $n > 1$, the steeper part of the knickpoint propagates faster and a knickpoint will become a concave-up knickzone with a steep upstream boundary mimicking a slope-break knickpoint. If $n < 1$, the opposite occurs and a knickpoint will progressively become a convex-up knickzone migrating upstream with a sharp downstream boundary (Lague, 2014). In this regard, to obtain the best mn ratio that in a linear context is equal to m, we applied the linear regression of the χ–z plot. In detail, the χ–z plot for every value of m from 0.1 to 1 and the coefficient of determination, or R^2, were computed, indicating −0.45 as the best solution (Figure 5).
2. A spatially constant K was assumed. The relation between upslope area A and stream gradient S along channels usually follows a power law (Di Biase & Whipple, 2011; Kirby & Whipple, 2012; Tucker & Whipple, 2002; Whipple & Tucker, 1999; Wobus et al., 2006), as described in Equation (3). It reveals the steady-state river profile from which it is possible to determine the k_{sn} value range. Such range is functional for the calibration of the K erodibility parameter used in river inversions. The best-fit power law was computed keeping fixed the concavity index at −0.45, as resulting from the linear regression shown in Figure 4b. The computation was performed using the "slopearea" function in the TopoToolbox (Schwanghart & Scherler, 2014). This function examines this relation using a stream network, a DEM (from which the stream gradient is derived), and the upslope area. The function aggregates gradient values into area bins (by default, 100 bins) and fits a power law. The confidence bounds for the fitting curve were set to 95%; the steepness index k_{sn} to 108.9 with a lower bound of 103.1 and an upper bound of 114.6 (Figure 6). In order to calibrate the erodibility K, we referred to the literature data for the axial zone of the Central Apennines (Bigi et al., 1995; D'Agostino et al., 2001; Girotti & Piccardi, 1994; Molin & Fubelli, 2005), which provided an average uplift rate ranging from 0.5 to 0.7 mm a^{-1}. In order to provide a sensitivity analysis on such a parameter, we estimated the maximum, mean, and minimum K, applying Equation (4), respectively, between the maximum uplift rate and the minimum k_{sn}, the mean uplift rate and the mean k_{sn}, the minimum uplift rate and the maximum k_{sn}. We found that $K_{max} = 6.79 \times 10^{-6}$ m$^{0.1}$ yr^{-1}, $K_{mean} = 5.51 \times 10^{-6}$ m$^{0.1}$ yr^{-1}, and $K_{min} = 4.36 \times 10^{-6}$ m$^{0.1}$ yr^{-1}.
3. Another key assumption of inversion modeling is that the drainage area of the fluvial channels remains fixed during the history that is represented by the long profiles of the rivers. Area change can take the form of stream piracy, migration of the main water divide, or migration of the lateral divides between the analyzed basins. In this regard, there is no evidence of river piracy in the study area.
4. Block uplift conditions were applied, which require space-invariant $U(t)$, but not necessarily steady state as shown in Equation (8). Such a scenario may apply, for example, in the case of linear rivers that flow perpendicular

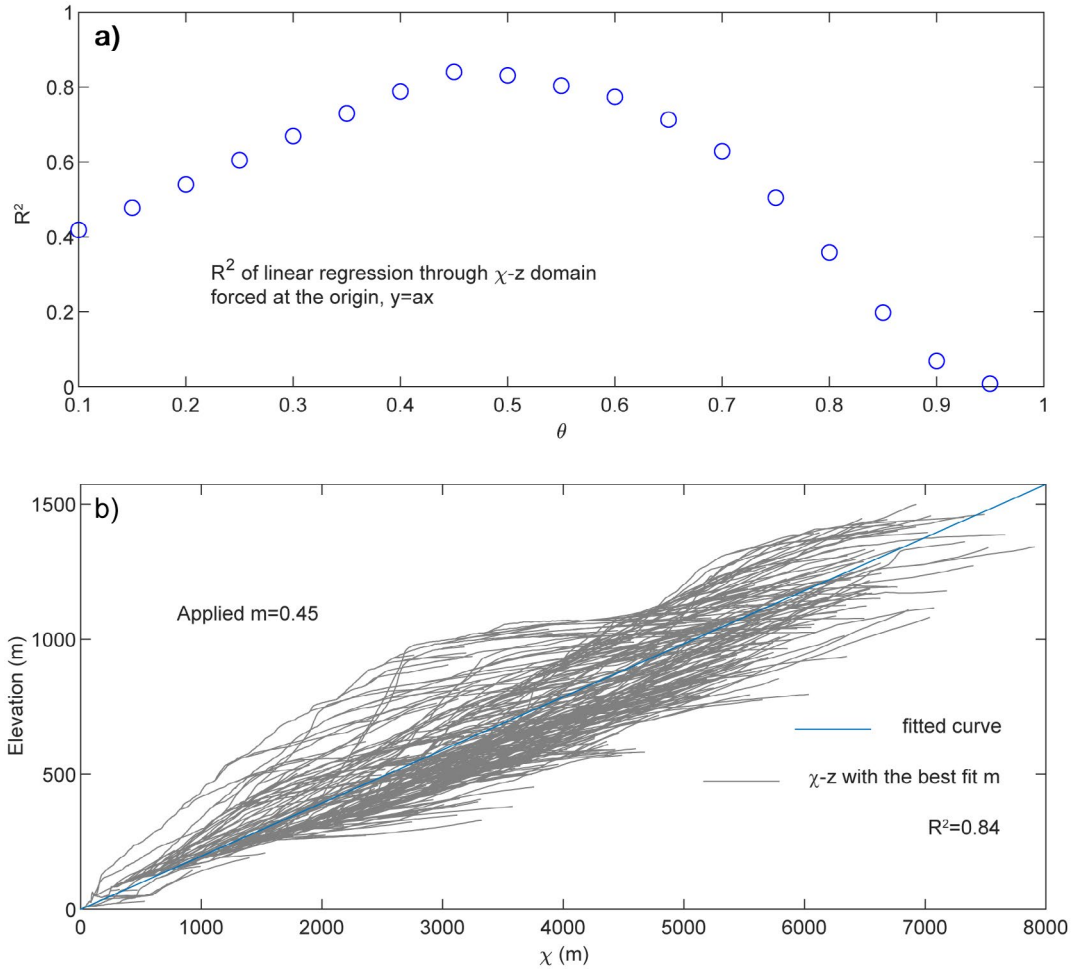

FIGURE 5 The "Linearize χ–z relationship" for identifying the *mn* ratio, or θ. The procedure varies the *mn* ratio until it finds a value that maximizes the linear correlation coefficient between the χ-transformed profile and a straight line. (a) Linear correlation coefficient versus *mn* ratio plot. (b) χ-transformed profile and a straight line with best fit *mn* ratio (0.45)

to a mountain range or when the source of uplift/base-level fall is localized at the outlet of the drainage basin, and U is unlikely to vary spatially across the region.

5.2 | Results

From the slope map of Figure 7, it is possible to note that the clastic deposits are associated with different levels of flat surfaces outcropping at several elevations, among which the most evident are the Campo dell'Osso, Camposecco, and Faito plateaus. Associated with the escarpments of the plateaus, the highest values of the k_{sn} index characterized the stream networks, while along the flat surfaces, they have low values. The knickpoints separated the upstream low-relief landscapes from the downstream steep valleys. In Figure 8, the stream network elevation was converted in τ space for the different values of K by applying Equation (7). Regarding the linear river inversion curves under the block uplift assumption, the tectonic histories that we generically interpret

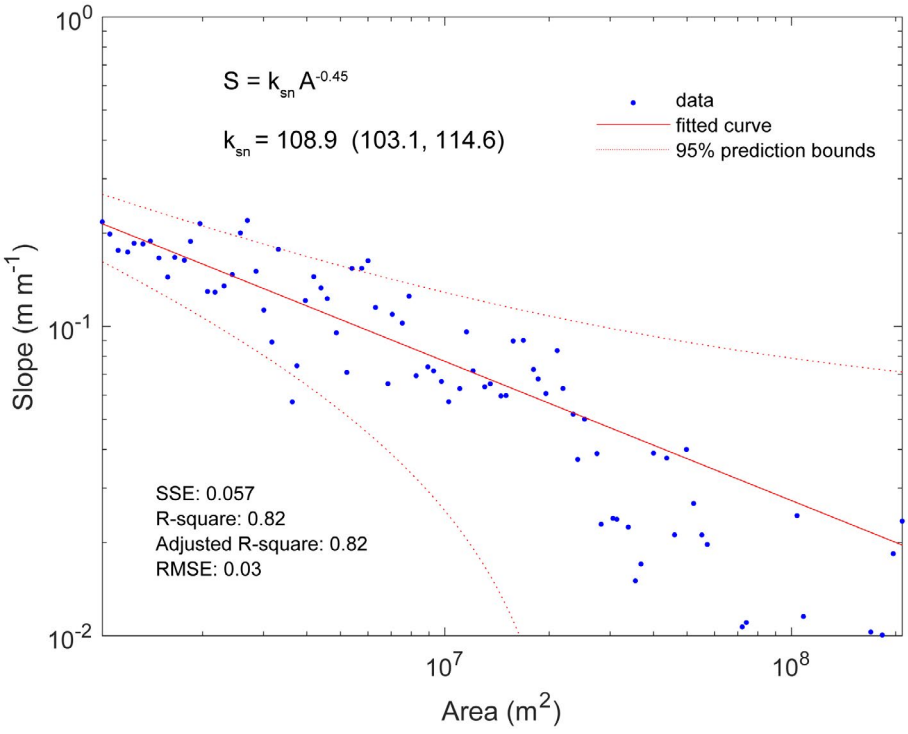

FIGURE 6 The slope–area plot of all the stream networks (including Simbrivio, Granara, and Campocatino sub-catchments) of the upper Aniene river basin. The *mn* ratio, or θ, is set fixed at −0.45 by the linear regression shown in Figure 4b. The confidence prediction bounds were set to 95%. The goodness-of-fit is expressed in SSE (sum of squared errors), R^2, adjusted R^2, and RMSE (root mean square error). The resulting k_{sn} range is used to calibrate the erodibility parameter

as base-level fall rate at the outlet point of the drainage system where the tectonic Simbruini range ends, are as longer as *K* is lower, with starting time of the tectonic record ranging from 1.9 Ma with K_{max} to 2.9 Ma with K_{min}. Moreover, the base-level fall rates are greater with increasing *K*.

The upper Aniene river valley records on average about 2.4 Ma of tectonic history. According to the average tectonic history in Figure 8, from 2.4 to 1.85 Ma, the base-level fall rate constantly increases, reaching a highest value of about 630 m Ma^{-1}. Then, from 1.85 to 0.76 Ma, it decreases except for a short period of time around 1 Ma when a slight increase is recorded. At 0.76 Ma the base-level fall rate reaches its minimum of about 360 m Ma^{-1} after which it rises again until the present, with a value of about 610 m Ma^{-1}.

5.3 | Misfit analysis

To apply the inversion scheme, we reconstructed the rate of uplift (or base-level fall) from the river network during discrete time intervals using Equation (8). The data are organized such that there are *N* data points of *z* and τ along the fluvial network that share a common uplift history and are ordered according to elevation. A time step of constant length, ΔT (0.010 Ma), is chosen that will determine the number of discrete time intervals *q*.

Using the discretization described above, Equation (8) can be written for each data point and the equations can be organized in matrix form:

$$\mathbf{AU} = \mathbf{z} \tag{10}$$

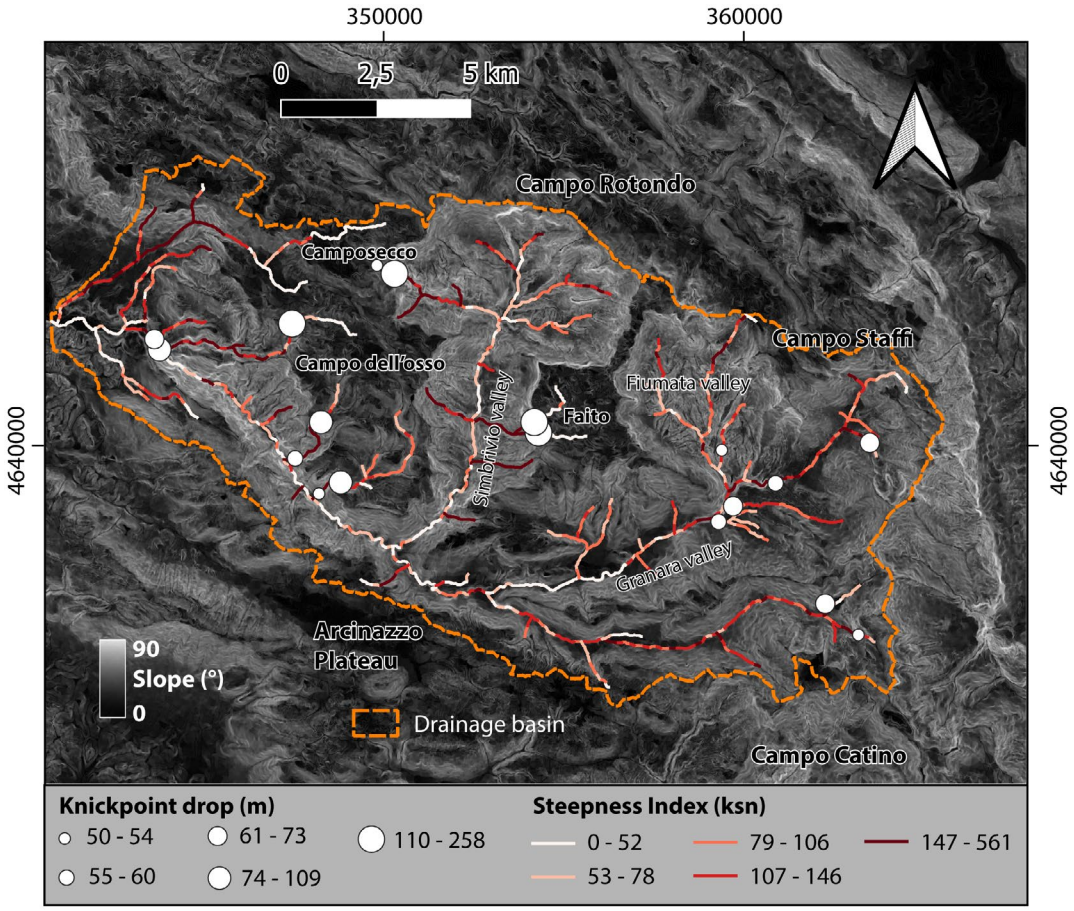

FIGURE 7 Slope map with k_{sn} values associated with the stream networks of the upper Aniene river basin (including Simbrivio, Granara, and Campocatino sub-catchments). The k_{sn} values were computed following Equation (3), keeping fixed the *mn* ratio, or θ, at −0.45, resulting from the linear regression shown in Figure 5. The coordinate system is WGS84-33N, EPSG: 32633. Both the slope map and the k_{sn} values are derived from the 10 m-resolution TINITALY DEM (Tarquini & Nannipieri, 2017)

where **A** is an $N \times q$ matrix, and **z** is elevation. This is an overdetermined inverse problem, as there are more known data points than unknown parameters. As such, a least-squares estimate for **U** is used (Tarantola, 1987):

$$\mathbf{U} = \mathbf{U}_{\mathbf{pri}} + \left(\mathbf{A}^{\mathrm{T}}\mathbf{A} + \Gamma^2\mathbf{I}\right)^{-1}\mathbf{A}^{\mathrm{T}}\left(\mathbf{z} - \mathbf{A}\mathbf{U}_{\mathbf{pri}}\right) \tag{11}$$

where

$$\mathbf{U}_{\mathbf{pri}} = \frac{1}{\mathrm{N}}\sum_{i=1}^{N}\left(\frac{z_i}{\sum_{j=1}^{q} A_{i,j}}\right) \tag{12}$$

is a prior guess at the uplift rate, Γ is a dampening coefficient that determines the smoothness imposed on the solution, and **I** is the $q \times q$ identity matrix. Since there are no independent constraints on the uplift rate before the start of the tectonic history recorded by the stream network, we have chosen to use the $\mathbf{U}_{\mathbf{pri}}$ values obtained through

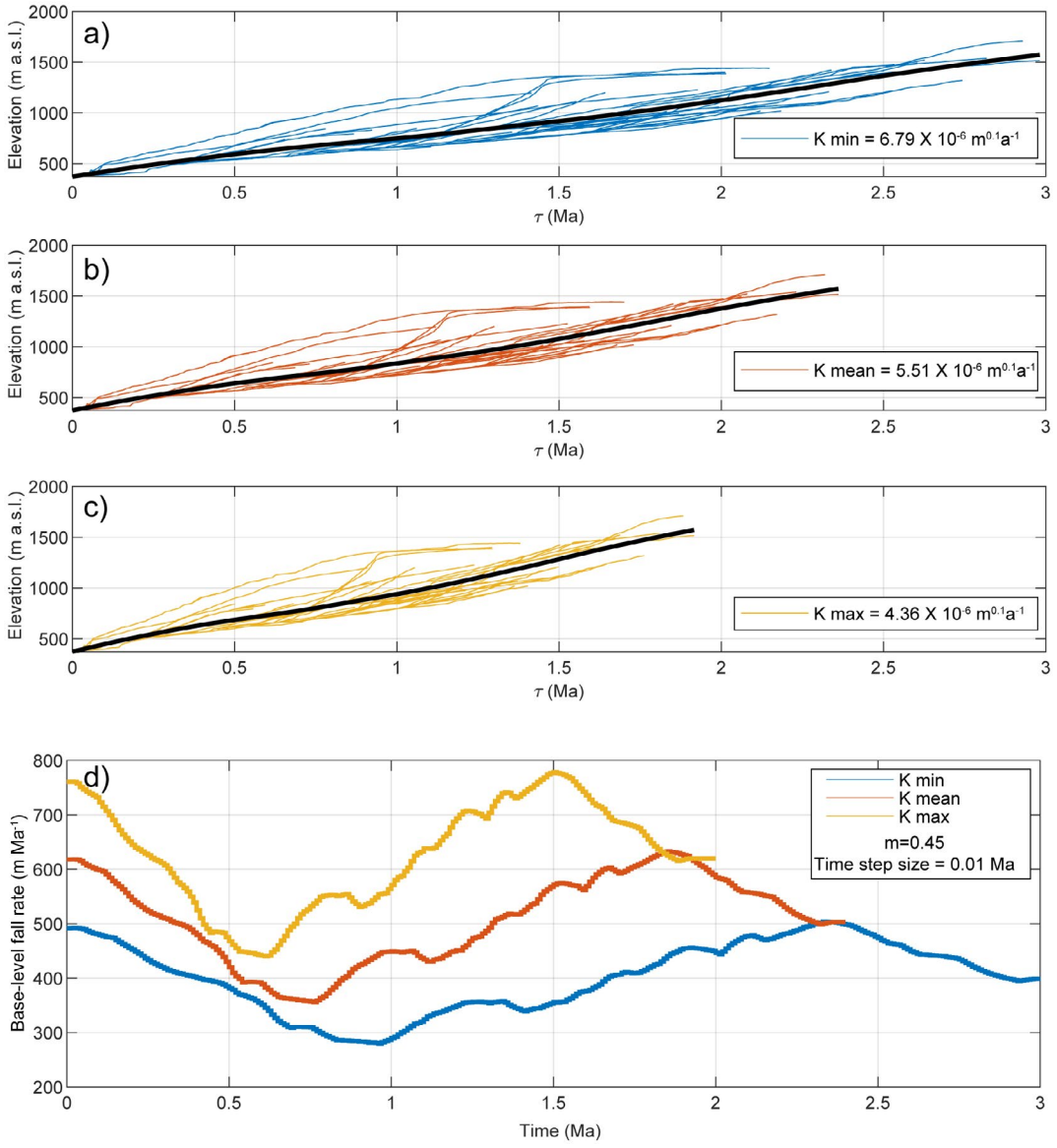

FIGURE 8 (a) Colored lines = empirical τ plots for the entire upper Aniene river basin. Black line = mean best-fit τ plots resulting from inverse modeling, where $m = 0.45$ and $K = K_{min}$. (b) As (a), but for $K = K_{mean}$. (c) As (a), but for $K = K_{max}$. (d) The linear river inversion curves describing the uplift rate histories, obtained for K_{max}, K_{mean}, and K_{min}. The parameters chosen in the modeling are described in the text and summarized in the panel

Equation (12), as described in Goren et al. (2014) and Gallen (2018). The computed values are 0.62, 0.5, and 0.4 mm a^{-1} for K_{max}, K_{mean}, and K_{min}, respectively.

We calculated the normalized misfit between the elevation of the pixels in the upper Aniene river basin, z_i, and the predicted elevations with the inferred uplift history, $\tilde{z}_i$:

$$\text{Misfit} = \frac{1}{N-M}\sqrt{\sum_{i=1}^{N}\left(z_i - \tilde{z}_i\right)^2} \tag{13}$$

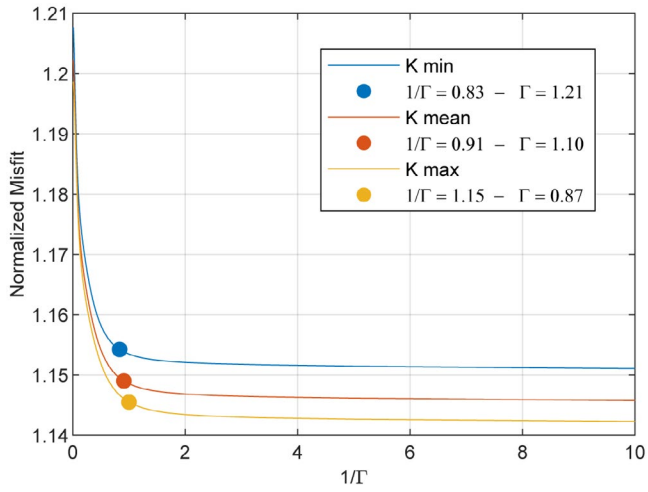

FIGURE 9 Normalized misfit [Equation (13)] as a function of $1/\Gamma$, where Γ is the dampening coefficient, computed for K_{max}, K_{mean}, and K_{min}. The points show the optimal inverse models for each erodibility parameter (Parker, 1994)

where N is the number of pixels of fluvial network data and $M = q$ is the number of discrete time intervals. Figure 9 shows the normalized misfit as a function of $1/\Gamma$ computed for three erodibility values K_{max}, K_{mean}, and K_{min}. The optimal solution is chosen at the corner of the normalized misfit versus $1/\Gamma$ relationship, or "L-curve" (Parker, 1994), highlighted by the points in Figure 8. We obtain values of Γ of 1.21, 1.10, and 0.87 for K_{max}, K_{mean}, and K_{min}, respectively.

6 | DISCUSSION

The Plio-Quaternary continental succession which crops out along the Simbruini–Ernici range was substantially unknown, being interpreted based on scattered and undetailed investigations as Miocene marine sediments, similar to the "Brecce della Renga" or, alternatively, Quaternary continental deposits (Beneo, 1938; Cavinato et al., 2012; Damiani, 1990; Devoto, 1967).

Although it is widely accepted that fluvial landscapes record temporal and spatial variations in rock uplift rates (Delchiaro et al., 2019; Fox et al., 2014; Gallen & Fernández-Blanco, 2021; Goren et al., 2014; Ma et al., 2020; Pritchard et al., 2009; Roberts & White, 2010; Rudge et al., 2015), a river-profile inverse model has not been applied to drainage in the region yet. Moreover, a precise evaluation of regional uplift rates in the Middle–Late Pleistocene is hampered by the relative scarcity of remnant shoreline deposits and uncertainties in their ages, especially on the Adriatic coast. Previous studies are only of limited use as long-term averages (Bigi et al., 1995; D'Agostino et al., 2001; Girotti & Piccardi, 1994; Molin & Fubelli, 2005).

Based on a new field survey of the continental deposits, on their plano-altimetric distribution and correlations and on the inverse modeling of the river longitudinal profiles, we were able to analyze both the erosional and the depositional phases which occurred in this sector of the central Apennines, from Pliocene to recent, and to better define the chronology of the continental deposits outcropping in the Simbruini Mts. (Figure 10).

The analysis focused on a complete drainage basin, the upper Aniene river basin, which shows no evidence of river captures. All the identified markers are associated with such a basin, so it can be assumed that the base-level changes, responsible for the origin of the deposits, influenced all the streams upstream of its outlet. Hence, the amount of error in the plano-altimetric correlations of geomorphic markers, associated with paleo-surfaces, is minimal, as well as the implication for the recovered uplift rates by which the interpretations are inferred.

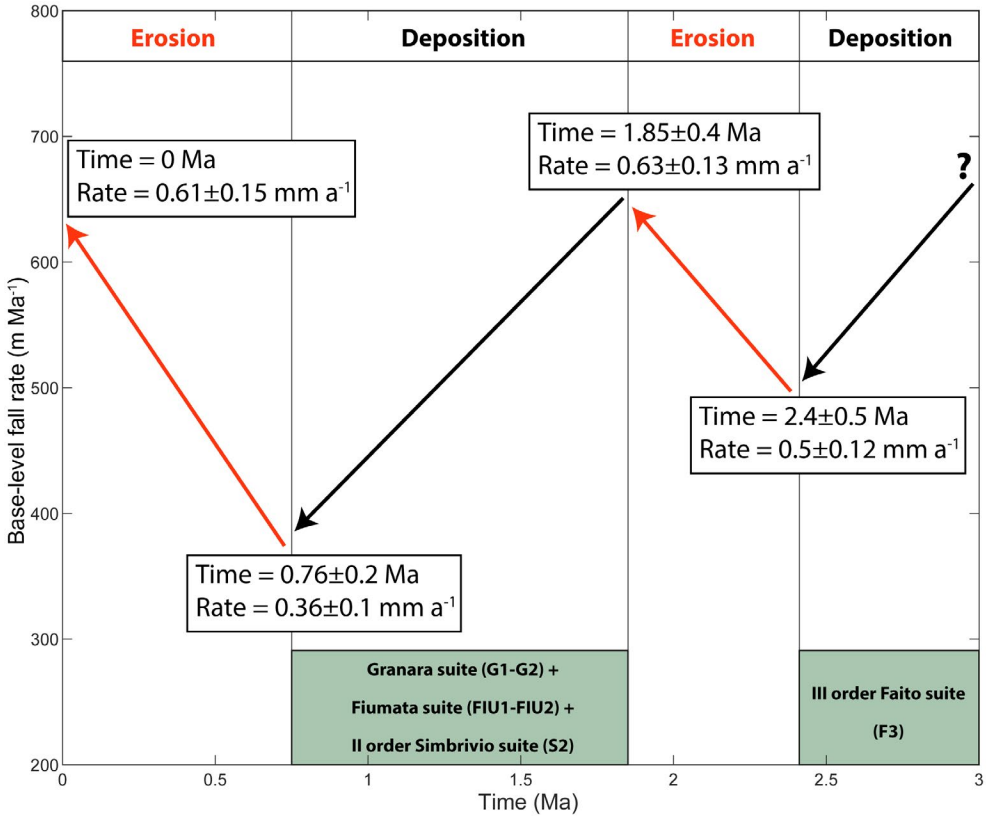

FIGURE 10 Synoptic diagram of the timing of Quaternary uplift in the Simbruini range. The main erosive and depositional phases (with errors) are reported, with which the emplacements of the clastic sequences and the relative base-level fall rates are associated

In the Simbrivio basin we identified the Faito suite (F1–F3) and the Simbrivio suite (S1, S2). The Simbrivio basin deposits are composed exclusively by carbonate clasts belonging to the Mesozoic Latium–Abruzzi platform, whereas they do not contain clasts belonging to Miocene carbonate units, siliciclastic foredeep deposits, which outcrop in the Roveto valley, Messinian "Puddinghe Poligeniche." The clasts which made up the Simbrivio deposits derive mostly from Cretaceous and, rarely, from Jurassic carbonate. The clast composition of the Faito units seems to reflect a progressive erosion and dismantling of the Simbruini stratigraphy. In fact, in the lower/older deposits (F1, F2, and S1 sub-units) we observe mostly Upper Cretaceous clasts and only in the upper/younger deposits do we observe a prevalence of dolostones, probably deriving from the Jurassic–Lower Cretaceous stratigraphy (F3). Moreover, from spatial distribution and geometrical relationships (vertical stacking of slope and conoidal facies) we determined that Faito clastic deposits were fed from the dismantling of reliefs located both to the north and south of the Faito plateau, and deposited onto a complex paleotopography, articulated in steep slopes and valleys. The F1–F3 sequence suggests the retrogradation of the depositional system, by the stacking of proximal (talus slope) F1 deposits and less proximal (alluvial fan) F2 and F3 facies. Afterwards, all the Faito clastic units were deeply incised and eroded during the erosional phase and a normal fault system dissected the entire structure, lowering the southwestern margin of the Faito plateau and leading to the complete disconnection of the deposits from their source area. From the Faito marker projections and the inverse modeling, we detected that the Faito suite should be deposited before 2.4 ± 0.5 Ma and was shaped by the first erosive phase between 2.4 ± 0.5 and 1.85 ± 0.4 Ma (Early Pleistocene), which fitted well with the survey data. In this time window, the uplift rate increased from 0.5 ± 0.12 to 0.63 ± 0.13 mm a^{-1}. Then the Faito clastic deposits: (1) deposited onto a relict surface

inherited from the last compressional phases (sealing the Vallepietra–Filettino line); (2) do not contain Miocene clasts (which would have been already eroded and re-sedimented in the "Brecce della Renga"); and (3) must have been deposited before the Lower Pleistocene erosive phase. On this basis, we suggest that the Faito units deposited during the Pliocene. The S1 unit is well correlated with the F2 unit, while S2 deposits lay at much lower elevation (but not as much as the Granara suite) and are therefore younger.

In the Granara and Fiumata basins, the morpho-stratigraphic relationships have been defined from geological surveys: in particular, differently from the Faito suite, in this area the older deposits lay scattered on the valley slopes (FIU1 and G1), while the younger deposits (FIU2 and G2) crop out at the bottom of the valleys, embedded in the older ones. From the Granara and Fiumata marker projections and the inverse modeling, we recognized a depositional phase followed by a new erosive phase, between 1.85 ± 0.4 and 0.76 ± 0.2 Ma (Early Pleistocene), and after 0.76 ± 0.2 Ma and still ongoing (Middle Pleistocene–present). In detail, the uplift rate first decreased from 0.63 ± 0.13 to 0.36 ± 0.1 mm a^{-1}, and then increased from 0.36 ± 0.1 to 0.61 ± 0.15 mm a^{-1}. Merging field data and geomorphometric analyses, we can suppose that FIU1 and G1 were deposited and eroded during the first phase, while FIU2 and G2 during the more recent phase. Furthermore, field survey data suggest that the G2 alluvial fan deposits are the only (among all those outcropping in the Simbruini sector) that contain clasts from the "Puddinghe Poligeniche," cropping out on the western slope of the Viglio Mt., a sector still connected with the present-day Granara valley morphology. The recent evolution of the Granara valley caused the involvement of the "Puddinghe Poligeniche" in the erosional phase, explaining the presence of "Puddinghe Poligeniche" clasts in G2 alluvial fan deposits.

7 | CONCLUSIONS

The application of morphometric analyses, together with detailed geological and geomorphological fieldwork, allowed us to shed light on the post-orogenic, Quaternary evolution of the Simbruini range (central Italy). Through the definition of the spatial distribution, clast content, depositional environment, and geometrical relationship of the continental clastic deposits, we were able to define their geometry and relative chronology.

Such data, together with the analyses of the plano-altimetric distribution of geomorphic markers and fluvial inverse modeling technique, offer new chronological insights into the identification of the depositional/erosional phases related to landscape evolution. This is of considerable relevance if we consider that these kind of continental clastic deposits are totally missing in absolute chronostratigraphic constraints.

Our results allow us to define the main phases of river incision and landscape erosion in the Simbruini area and to constrain, for the first time, the chronology of the different generations of continental clastic units, which are the only deposits recording the post-orogenic evolution of this key sector of the Central Apennines. Our findings are the necessary premise for comparing the history of the main Central Apennines reliefs with that of the post-orogenic intermontane sedimentary basins and, ultimately, understanding the long-term morphotectonic and climatic evolution of this sector of the Apennines.

ACKNOWLEDGMENTS

The research was carried out as part of the PhDs of Michele Delchiaro in Earth Sciences at Sapienza University of Rome and Veronica Fioramonti in Earth Sciences at Roma Tre University of Rome, respectively. This study has been funded by Italian MIUR through PRIN_2015 (project 20158A9CBM_002) grant to MM and Department of Science (Roma TRE University, Dipartimento di Eccellenza, Art. 1, com. 314-337, Legge 232/2016) grants. We are also grateful to Simone Fabbi and two anonymous reviewers for their deep and stimulating revision of the manuscript, as well as to the editorial work by the Guest Editor Massimiliano Alvioli and the Editor John Wilson. Open Access Funding enabled and organized by Universita degli Studi di Roma La Sapienza within the CRUI-CARE Agreement.

CONFLICT OF INTEREST

The authors declare no conflict of interest.

DATA AVAILABILITY STATEMENT

The data that support the findings of this study are available from the corresponding author upon reasonable request.

ORCID

Michele Delchiaro https://orcid.org/0000-0002-0843-1003

REFERENCES

Accordi, B. (1966). La componente traslativa nella tettonica dell'Appennino laziale-abruzzese. *Geologica Romana*, *5*, 355–406.

Accordi, B., Devoto, G., La Monica, G. B., Praturlon, A., Sirna, G., & Zalaffi, M. (1967). Il Neogene nell'Appennino laziale-abruzzese: Committee Mediterranean Neogene Stratigraphy, Proc. IV Session, Bologna. *Giornale di Geologia*, *35*, 235–268.

Accordi, G., & Carbone, F. (Eds.). (1986). Lithofacies map of Latium-Abruzzi and neighboring areas (Scale 1:250,000). *Quaderni De La Ricerca Scientifica*, *114*(5), 7–215.

Bally, A. W. (1986). Balanced sections and seismic reflection profiles across the Central Apennines. *Memorie Società geologico d'italia*, *35*, 257–310.

Beneo, E. (1938). Appunti geologici sulle regioni dell'Appennino centrale comprese nel Foglio (Alatri). *Bollettino del R. Comitato geologico d'italia*, *63*, 1–75.

Bieler-Chatelan, T. (1928). Gli antichi ghiacciai pleistocenici dei Monti Simbruini (Appennino Centrale). *Bollettino della Società geologica italiana*, *47*(1), 33–45.

Bieler-Chatelan, T. (1929). Nuove osservazioni sulle tracce glaciali dei Monti Simbruini (Appennino Centrale). *Bollettino della Società geologica italiana*, *48*(1), 163–175.

Bigi, S., Cantalamessa, G., Centamore, E., Didaskalou, P., Dramis, F., Farabollini, P., … Potetti, M. (1995). La fascia periadriatica marchigiano-abruzzese dal Pliocene medio ai tempi attuali: Evoluzione tettonico-sedimentaria e geomorfologica. *Studi geologici camerti*, *n. special*, *2*, 37–49.

Bosi, C., & Messina, P. (1990). Elementi di stratigrafia neogenico-quaternaria tra il Fucino e la valle del Giovenco (L'Aquila). *Memorie Descrittive della Carta Geologica d'italia*, *38*, 85–96.

Brandano, M. (2002). La Formazione dei "Calcari a Briozoi e Litotamni" nell'area di Tagliacozzo (Appennino centrale) e considerazioni paleoambientali sulle facies rodalgali. *Bollettino della Società geologica italiana*, *121*, 179–186.

Calamita, F., Di Domenica, A., Viandante, M. G., & Tavarnelli, E. (2008). Sovrascorrimenti younger on older o faglie normali ruotate: La linea Vallepietra-Filettino-Monte Ortara (Appennino centrale laziale-abruzzese). *Rendiconti Online della Società Geologica Italiana*, *1*, 43–47.

Carminati, E., Corda, L., Mariotti, G., & Brandano, M. (2007). Tectonic control on the architecture of a Miocene carbonate ramp in the Central Apennines (Italy): Insights from facies and backstripping analyses. *Sedimentary Geology*, *198*(3–4), 233–253. https://doi.org/10.1016/j.sedgeo.2006.12.005

Carminati, E., Fabbi, S., & Santantonio, M. (2014). Slab bending, syn-subduction normal faulting, and out-of-sequence thrusting in the Central Apennines. *Tectonics*, *33*(4), 530–551. https://doi.org/10.1002/2013TC003386

Carminati, E., Lustrino, M., Cuffaro, M., & Doglioni, C. (2010). Tectonics, magmatism and geodynamics of Italy: What we know and what we imagine. *Journal of the Virtual Explorer*, *36*, 9. https://doi.org/10.3809/jvirtex.2010.00226

Castellarin, A., Colacicchi, R., & Praturlon, A. (1978). Fasi distensive, trascorrenze e sovrascorrimenti lungo la "Linea Ancona-Anzio", dal Lias medio al Pliocene. *Geologica Romana*, *17*, 161–189.

Cavinato, G. P., Corrado, S., & Sirna, M. (1993). Geometrie ed evoluzione cinematica del settore centrale della catena Simbruino-Ernica (Lazio, Appennino centrale). *Geologica Romana*, *29*, 435–453.

Cavinato, G. P., & DeCelles, P. (1999). Extensional basins in the tectonically bimodal central Apennines fold-thrust belt, Italy: Response to corner flow above a subducting slab in retrograde motion. *Geology*, *27*(10), 955–958. https://doi.org/10.1130/0091-7613(1999)027<0955:EBITTB>2.3.CO;2

Cavinato, G. P., Parotto, M., & Sirna, M. (2012). I Monti Ernici: Da peripheral bulge a orogeno. Stato dell'arte della ricerca. *Rendiconti Online della Società Geologica Italiana*, *23*, 31–44.

Chiocchini, M., Chiocchini, R. A., Didaskalou, P., & Potetti, M. (2008). Microbiostratigrafia del Triassico superiore, Giurassico e Cretacico in facies di piattaforma carbonatica del Lazio centro meridionale e Abruzzo: Revisione finale. *Memorie Descrittive della Carta Geologica d'italia*, *84*, 5–170.

Cipollari, P., & Cosentino, D. (1991). La linea Olevano-Antrodoco: Contributo della biostratigrafia alla sua caratterizzazione cinematica. *Studi Geologici Camerti, v. speciale*, *2*, 143–149.

Cipollari, P., & Cosentino, D. (1993). Le Arenarie di Torrice: Un deposito di bacino di piggy-back del Messiniano nell'Appennino centrale. *Bollettino della Società Geologica Italiana*, *112*(2), 497–505.

Cipollari, P., & Cosentino, D. (1995). Miocene unconformities in the Central Apennines: Geodynamic significance and sedimentary basin evolution. *Tectonophysics*, *252*(1–4), 375–389. https://doi.org/10.1016/0040-1951(95)00088-7

Cipollari, P., & Cosentino, D. (1999). Cronostratigrafia dei depositi neogenici del settore ernico simbruino, Appennino centrale. *Bollettino della Società Geologica Italiana*, *118*(2), 439–459.

Cipollari, P., Cosentino, D., Esu, D., Girotti, O., Gliozzi, E., & Praturlon, A. (1999). Thrust-top lacustrine–lagoonal basin development in accretionary wedges: Late Messinian (Lago-Mare) episode in the central Apennines (Italy). *Palaeogeography, Palaeoclimatology, Palaeoecology*, *151*(1–3), 149–166. https://doi.org/10.1016/S0031-0182(99)00026-7

Civitelli, G., & Brandano, M. (2005). Atlante delle litofacies e modello deposizionale dei Calcari a Briozoi e Litotamni nella Piattaforma carbonatica laziale-abruzzese. *Bollettino della Società Geologica Italiana*, *124*(3), 611.

Compagnoni, B., Galluzzo, F., & Santantonio, M. (1990). Le «Brecce della Renga» (M. ti Simbruini): Un esempio di sedimentazione controllata dalla tettonica. *Memorie Descrittive della Carta Geologica d'italia*, *38*, 59–76.

Cosentino, D., Asti, R., Nocentini, M., Gliozzi, E., Kotsakis, T., Mattei, M., … Pennacchioni, M. (2017). New insights into the onset and evolution of the central Apennines extensional intermontane basins based on the tectonically active L'Aquila Basin (central Italy). *Geological Society of America Bulletin*, *129*(9–10), 1314–1336. https://doi.org/10.1130/B31679.1

Cosentino, D., Cipollari, P., Marsili, P., & Scrocca, D. (2010). Geology of the central Apennines: A regional review. *Journal of the Virtual Explorer*, *36*(11), 1–37. https://doi.org/10.3809/jvirtex.2009.00223

Critelli, S., Le Pera, E., Galluzzo, F., Milli, S., Moscatelli, M., Perrotta, S., & Santantonio, M. (2007). Interpreting siliciclastic-carbonate detrital modes in foreland basin systems: An example from Upper Miocene arenites of the central Apennines, Italy. *Special Papers of the Geological Society of America*, *420*, 107. https://doi.org/10.1130/2006.2420(08)

D'Agostino, N., Jackson, J. A., Dramis, F., & Funiciello, R. (2001). Interactions between mantle upwelling, drainage evolution and active normal faulting: An example from the central Apennines (Italy). *Geophysical Journal International*, *147*(2), 475–497. https://doi.org/10.1046/j.1365-246X.2001.00539.x

Damiani, A. V. (1990). Considerations and problems on tectonic and paleogeologic Simbruini Mts. *Memorie Descrittive della Carta Geologica d'italia*, *38*, 177–206.

Damiani, A. V., Catenacci, V., Molinari, V., Panseri, C., & Tilia, A. (1998). *Note illustrative del F. 376 SUBIACO (scala 1:50,000)*. Ispra, Italy: Servizio Geologico Nazionale, Istituto Poligrafico e Zecca dello Stato.

Damiani, A. V., Catenacci, V., Molinari, V., & Pichezzi, R. M. (1991). Lito-biofacies del Triassico superiore-Dogger nei Monti Simbruini e nei Monti Ernici (Lazio). *Studi geologici camerti, n. speciale*, *1991*, 181–186.

Damiani, A. V., & Pannuzi, L. (1976). La glaciazione wurmiana nell'Appennino laziale abruzzese. *Bollettino della ocietà Geologica Italiana*, *97*, 85–106.

Damiani, A. V., & Pannuzi, L. (1980). La neotettonica del Foglio 153 "Agnone". *Progetto Finalizzato Geodinamica*, *356*, 237–248.

Damiani, A. V., & Pannuzi, L. (1990). La glaciazione pleistocenica nell'Appennino laziale abruzzese: Nota V, I ghiacciaii dei monti Simbruini (Campo Ceraso, Valle Mozzone, Fiumata, Valle Granara) e considerazioni di tettonica recente. *Memorie Descrittive della Carta Geologica d'italia*, *38*, 215–250.

Delchiaro, M., Della Seta, M., Martino, S., Dehbozorgi, M., & Nozaem, R. (2019). Reconstruction of river valley evolution before and after the emplacement of the giant Seymareh rock avalanche (Zagros Mts., Iran). *Earth Surface Dynamics*, *7*(4), 929–947. https://doi.org/10.5194/esurf-7-929-2019

Devoto, G. (1967a). Note geologiche sul settore centrale dei Monti Simbruini ed Ernici (Lazio nord-orientale). *Bollettino della Società dei Naturalisti in Napoli*, *76*, 1–112.

Devoto, G. (1967b). Le brecce calcaree mioceniche nell'alta Valle Roveto, fra Castellafiume e Canistro (Frosinone, Lazio meridionale). *Geologica Romana*, *6*, 75–86.

Devoto, G. (1970). Sguardo geologico dei Monti Simbruini (Lazio nord-orientale). *Geologica Romana*, *9*, 127–136.

Devoto, G., & Parotto, M. (1967). Note geologiche sui rilievi tra Monte Crepacuore e Monte Ortara (Monti Ernici-Lazio nord-orientale). *Geologica Romana*, *6*, 145–163.

Di Biase, R. A., & Whipple, K. X. (2011). The influence of erosion thresholds and runoff variability on the relationships among topography, climate, and erosion rate. *Journal of Geophysical Research: Earth Surface*, *116*, F04036. https://doi.org/10.1029/2011JF002095

Doglioni, C., Moretti, I., & Roure, F. (1991). Basal lithospheric detachment, eastward mantle flow and Mediterranean geodynamics: A discussion. *Journal of Geodynamics*, *13*(1), 47–65. https://doi.org/10.1016/0264-3707(91)90029-E

Dondi, L., Papetti, I., & Tedeschi, D. (1966). Stratigrafia del pozzo Trevi 1 (Lazio). *Geologica Romana*, *5*, 249–262.

D'Orefice, M., Graciotti, R., Chiessi, V., Neri, P. C., Morri, A., Roma, M., & Falcetti, S. (2014). La conca intermontana di Oricola-Carsoli (AQ): Caratteri geologici, geomorfologici e applicativi. *Memorie Descrittive della Carta Geologica d'italia*, *91*, 7–114.

Elter, P., Giglia, G., Tongiorgi, M., & Trevisan, L. (1975). Tensional and compressional areas in the recent (Tortonian to present) evolution of the Northern Apennines. *Bollettino di Geofisica Teorica ed Applicata*, *17*, 3–18.

Fabbi, S. (2012). Late Miocene extension in the Central Apennines: Field evidence from the Simbruini Mts. *Rendiconti Online Societa Geologica Italiana*, *21*, 89–91.

Fabbi, S. (2016). Geology of the Northern Simbruini Mts. (Abruzzo-Italy). *Journal of Maps*, *12*(Suppl. 1), 441–452. https://doi.org/10.1080/17445647.2016.1237899

Fabbi, S. (2018). Geology of the eastern slopes of the Simbruini Mts. between Verrecchie and Capistrello (Central Apennines-Abruzzo. Italy). *Journal of Maps*, *14*(2), 435–446. https://doi.org/10.1080/17445647.2018.1483843

Fabbi, S., Galluzzo, F., Pichezzi, R. M., & Santantonio, M. (2014). Carbonate intercalations in a terrigenous foredeep: Late Miocene examples from the Simbruini Mts. and the Salto Valley (Central Apennines-Italy). *Italian Journal of Geosciences*, *133*(1), 85–100. https://doi.org/10.3301/IJG.2013.13

Fabbi, S., & Rossi, M. (2014). The Brecce della Renga Formation: Age and sedimentology of a syn-tectonic clastic unit in the upper Miocene of Central Apennines. Insights from field geology. *Rivista Italiana di Paleontologia e Stratigrafia*, *120*(2), 225–242.

Fabbi, S., & Santantonio, M. (2019). First report of a Messinian coralgal facies in a terrigenous setting of Central Apennines (Italy) and its palaeogeographic significance. *Geological Journal*, *54*(3), 1756–1768. https://doi.org/10.1002/gj.3267

Finnegan, N. J., Sklar, L. S., & Fuller, T. K. (2007). Interplay of sediment supply, river incision, and channel morphology revealed by the transient evolution of an experimental bedrock channel. *Journal of Geophysical Research: Earth Surface*, *112*, F03S11. https://doi.org/10.1029/2006JF000569

Forte, A. M., & Whipple, K. X. (2019). The topographic analysis kit (TAK) for TopoToolbox. *Earth Surface Dynamics*, *7*, 87–95. https://doi.org/10.5194/esurf-7-87-2019

Fox, M., Goren, L., May, D. A., & Willett, S. D. (2014). Inversion of fluvial channels for paleorock uplift rates in Taiwan. *Journal of Geophysical Research: Earth Surface*, *119*(9), 1853–1875. https://doi.org/10.1002/2014JF003196

Funiciello, R., & Parotto, M. (1978). Il substrato sedimentario nell'area dei Colli Albani: Considerazioni geodinamiche e paleogeografiche sul margine tirrenico dell'Appenino Centrale. *Geologica Romana*, *17*, 233–287.

Gallen, S. F. (2018). Lithologic controls on landscape dynamics and aquatic species evolution in post-orogenic mountains. *Earth and Planetary Science Letters*, *493*, 150–160. https://doi.org/10.1016/j.epsl.2018.04.029

Gallen, S. F., & Fernández-Blanco, D. (2021). A new data-driven Bayesian inversion of fluvial topography clarifies the tectonic history of the Corinth rift and reveals a channel steepness threshold. *Journal of Geophysical Research: Earth Surface*, *126*(3), e2020JF005651. https://doi.org/10.1029/2020JF005651

Ghisetti, F., & Vezzani, L. (1997). Interfering paths of deformation and development of arcs in the fold-and-thrust belt of the central Apennines (Italy). *Tectonics*, *16*(3), 523–536. https://doi.org/10.1029/97TC00117

Giaccio, B., Leicher, N., Mannella, G., Monaco, L., Regattieri, E., Wagner, B., … Tzedakis, P. C. (2019). Extending the tephra and palaeoenvironmental record of the Central Mediterranean back to 430 ka: A new core from Fucino Basin, central Italy. *Quaternary Science Reviews*, *225*, 106003. https://doi.org/10.1016/j.quascirev.2019.106003

Giaccio, B., Regattieri, E., Zanchetta, G., Wagner, B., Galli, P., Mannella, G., … Cavinato, G. P. (2015). A key continental archive for the last 2 Ma of climatic history of the central Mediterranean region: A pilot drilling in the Fucino Basin, central Italy. *Scientific Drilling*, *20*, 13. https://doi.org/10.5194/sd2720-13-2015

Girotti, O., & Piccardi, E. (1994). Linee di riva del Pleistocene inferiore sul versante sinistro della Media Valle del fiume Tevere. *Il Quaternario*, *7*, 525–536.

Goren, L., Fox, M., & Willett, S. D. (2014). Tectonics from fluvial topography using formal linear inversion: Theory and applications to the Inyo Mountains, California. *Journal of Geophysical Research: Earth Surface*, *119*(8), 1651–1681. https://doi.org/10.1002/2014JF003079

Howard, A. D., & Kerby, G. (1983). Channel changes in badlands. *Geological Society of America Bulletin*, *94*(6), 739–752. https://doi.org/10.1130/0016-7606(1983)94<739:CCIB>2.0.CO;2

Jaurand, E. (1994). Découverte de nouvelles moraines faillées dans l'Apennin central (Italie) [Discovery of new faulted moraines in the central Apennines (Italy)]. *Bulletin de l'association de géographes français*, *71*(1), 73–84. https://doi.org/10.3406/bagf.1994.1721

Kastens, K. A., & Mascle, J. (1990). The geological evolution of the Tyrrhenian Sea: An introduction to the scientific results of ODP Leg 107. In K. A. Kastens & J. Mascle (Eds.), *Proceedings of the ocean drilling program, scientific results* (Vol. *107*, p. 26). College Station, TX: Ocean Drilling Program. https://doi.org/10.2973/odp.proc.sr.107.187.1990

Kirby, E., & Whipple, K. X. (2012). Expression of active tectonics in erosional landscapes. *Journal of Structural Geology*, *44*, 54–75. https://doi.org/10.1016/j.jsg.2012.07.009

Lague, D. (2014). The stream power river incision model: Evidence, theory and beyond. *Earth Surface Processes and Landforms*, *39*(1), 38–61. https://doi.org/10.1002/esp.3462

Larsen, I. J., & Montgomery, D. R. (2012). Landslide erosion coupled to tectonics and river incision. *Nature Geoscience*, *5*(7), 468–473. https://doi.org/10.1038/ngeo1479

Lavecchia, G., Brozzetti, F., Barchi, M., Menichetti, M., & Keller, J. V. (1994). Seismotectonic zoning in east-central Italy deduced from an analysis of the Neogene to present deformations and related stress fields. *Geological Society of America Bulletin*, *106*(9), 1107–1120. https://doi.org/10.1130/0016-7606(1994)106<1107:SZIECI>2.3.CO;2

Ma, Z., Zhang, H., Wang, Y., Tao, Y., & Li, X. (2020). Inversion of Dadu River bedrock channels for the Late Cenozoic uplift history of the eastern Tibetan Plateau. *Geophysical Research Letters*, *47*(4), e2019GL086882. https://doi.org/10.1029/2019GL086882

Malinverno, A., & Ryan, W. B. (1986). Extension in the Tyrrhenian Sea and shortening in the Apennines as result of arc migration driven by sinking of the lithosphere. *Tectonics*, *5*(2), 227–245. https://doi.org/10.1029/TC005i002p00227

Martinis, B., & Pieri, M. (1964). Alcune notizie sulla formazione evaporitica dell'Italia centrale e meridionale. *Memorie Societa Geologica Italiana*, *4*, 649–678.

Milli, S., & Moscatelli, M. (2000). Facies analysis and physical stratigraphy of the Messinian turbiditic complex in the Valle del Salto and Val di Varri (Central Apennines). *Giornale di Geologia*, *62*, 57–77.

Molin, P., & Fubelli, G. (2005). Morphometric evidence of the topographic growth of the Central Apennines. *Geografia Fisica e Dinamica Quaternaria*, *28*(3), 47–61.

Montgomery, D. R., & Brandon, M. T. (2002). Topographic controls on erosion rates in tectonically active mountain ranges. *Earth and Planetary Science Letters*, *201*(3–4), 481–489. https://doi.org/10.1016/S0012-821X(02)00725-2

Naso, G., Parotto, M., Tallini, M., & Tozzi, M. (1992). Mecanismi transpressivi nell'Appennino centrale: La linea Vallepietra-Filettino (Monti Simbruini, Lazio). *Bollettino della Società Geologica Italiana*, *111*(2), 163–179.

Parker, R. L. (1994). *Geophysical inverse theory* (Vol. *1*). Princeton, NJ: Princeton University Press.

Parotto, M. (1971). Stratigraphy and tectonics of the eastern Simbruini and western Marsica ranges (Central Apennines, Italy). *Accademia dei Lincei*, *9*, 93–170.

Parotto, M. (1980). L'Apennin central. *Introduction ala géologie generale d'italie*, *26*, 33–37.

Parotto, M., & Praturlon, A. (1975). Geological summary of Central Apennines: Quaderni de Idquo La ricerca scientifica rdquo. *Consiglio Nazionale delle Ricerche*, *90*, 257–311.

Parotto, M., & Praturlon, A. (2004). The southern Apennines arc. In V. Crescenti, S. D'Offizí, S. Merhino, & L. Sacchi (Eds.), *Geology of Italy: Special volume of the Italian Geological Society for the IGC 32 Florence-2004* (pp. 33–58). Rome, Italy: Italian Geological Society.

Pasquali, V., Castorina, F., Cipollari, P., Cosentino, D., & Lo Mastro, S. (2007). I depositi tardo-orogenici della Valla Latina meridionale: Stratigrafia e implicazioni cinematiche per l'evoluzione dell'Appennino centrale. *Bollettino della Società Geologica Italiana*, *126*(1), 101–118.

Patacca, E., & Scandone, P. (1987). *Tectonic evolution of the outer margin of the Apennines and related foredeep system* (Unpublished report).

Patacca, E., & Scandone, P. (1989). Post-Tortonian mountain building in the Apennines. The role of the passive sinking of a relic lithospheric slab. *Accademia Nazionale dei Lincei*, *80*, 157–176.

Patacca, E., Scandone, P., Di Luzio, E., Cavinato, G. P., & Parotto, M. (2008). Structural architecture of the central Apennines: Interpretation of the CROP 11 seismic profile from the Adriatic coast to the orographic divide. *Tectonics*, *27*, TC3006. https://doi.org/10.1029/2005TC001917

Perron, J. T., & Royden, L. (2013). An integral approach to bedrock river profile analysis. *Earth Surface Processes and Landforms*, *38*(6), 570–576. https://doi.org/10.1002/esp.3302

Pieri, M. (1966). Tentativo di ricostruzione paleogeografico-strutturale dell'Italia centro21 meridionale. *Geologica Romana*, *5*(4), 407–424.

Pritchard, D., Roberts, G. G., White, N. J., & Richardson, C. N. (2009). Uplift histories from river profiles. *Geophysical Research Letters*, *36*, L24301. https://doi.org/10.1029/2009GL040928

Roberts, G. G., & White, N. (2010). Estimating uplift rate histories from river profiles using African examples. *Journal of Geophysical Research: Solid Earth*, *115*, B02406. https://doi.org/10.1029/2009JB006692

Roering, J. J., Perron, J. T., & Kirchner, J. W. (2007). Functional relationships between denudation and hillslope form and relief. *Earth and Planetary Science Letters*, *264*(1–2), 245–258. https://doi.org/10.1016/j.epsl.2007.09.035

Rudge, J. F., Roberts, G. G., White, N. J., & Richardson, C. N. (2015). Uplift histories of Africa and Australia from linear inverse modeling of drainage inventories. *Journal of Geophysical Research: Earth Surface*, *120*(5), 894–914. https://doi.org/10.1002/2014JF003297

Sartori, R. (1990). The main results of ODP Leg 107 in the frame of Neogene to Recent geology of peri-Tyrrhenian areas. In K. A. Kastens & J. Mascle (Eds.), *Proceedings of the Ocean Drilling Program: Scientific results* (Vol. *107*, pp. 715–730). College Station, TX: Ocean Drilling Program. https://doi.org/10.2973/odp.proc.sr.107.183.1990

Schwanghart, W., & Scherler, D. (2014). TopoToolbox 2—MATLAB-based software for topographic analysis and modeling in Earth surface sciences. *Earth Surface Dynamics*, *2*(1), 1–7. https://doi.org/10.5194/esurf-2-1-2014

Tarantola, A. (1987). *Inverse problem theory: Methods for data fitting and model parameter estimation*. Philadelphia, PA: Society for Industrial and Applied Mathematics.

Tarquini, S., & Nannipieri, L. (2017). The 10 m-resolution TINITALY DEM as a trans-disciplinary basis for the analysis of the Italian territory: Current trends and new perspectives. *Geomorphology*, *281*, 108–115. https://doi.org/10.1016/j.geomorph.2016.12.022

Tucker, G. E., & Whipple, K. X. (2002). Topographic outcomes predicted by stream erosion models: Sensitivity analysis and intermodel comparison. *Journal of Geophysical Research: Solid Earth*, *107*(B9), ETG-1. https://doi.org/10.1029/2001JB000162

Whipple, K. X., & Tucker, G. E. (1999). Dynamics of the stream-power river incision model: Implications for height limits of mountain ranges, landscape response timescales, and research needs. *Journal of Geophysical Research: Solid Earth*, *104*(B8), 17661–17674. https://doi.org/10.1029/1999JB900120

Whittaker, A. C., Cowie, P. A., Attal, M., Tucker, G. E., & Roberts, G. P. (2007). Contrasting transient and steady-state rivers crossing active normal faults: New field observations from the Central Apennines, Italy. *Basin Research*, *19*(4), 529–556. https://doi.org/10.1111/j.1365-2117.2007.00337.x

Willett, S. D., Slingerland, R., & Hovius, N. (2001). Uplift, shortening, and steady state topography in active mountain belts. *American Journal of Science*, *301*(4–5), 455–485. https://doi.org/10.2475/ajs.301.4-5.455

Wobus, C., Whipple, K. X., Kirby, E., Snyder, N., Johnson, J., Spyropolou, K., … Sheehan, D. (2006). Tectonics from topography: Procedures, promise, and pitfalls. *Special Papers of the Geological Society of America*, *398*, 55–74.

How to cite this article: Delchiaro, M., Fioramonti, V., Della Seta, M., Paolo Cavinato, G., & Mattei, M. (2021). Fluvial inverse modeling for inferring the timing of Quaternary uplift in the Simbruini range (Central Apennines, Italy). *Transactions in GIS*, 00, 1–26. https://doi.org/10.1111/tgis.12833